


AUTHOR QUERY FORM

 <p>ELSEVIER</p>	<p>Journal : NLM</p> <p>Article Number : 1606</p>	<p>Please e-mail or fax your responses and any corrections to:</p> <p>E-mail: corrections.eseo@elsevier.macipd.com</p> <p>Fax: +44 1392 285878</p>
---	---	---

Dear Author,

During the preparation of your manuscript for typesetting, some questions may have arisen. These are listed below and highlighted by flags in the margin of the proof. Please check your typeset proof carefully and mark any corrections in the margin of the proof or compile them as a separate list. In case artwork needs revision, please consult <http://www.elsevier.com/artworkinstructions>

Electronic file usage

Sometimes we are unable to process the electronic file of your article and/or artwork. If this is the case, we have proceeded by:

- Scanning (parts of) your article
 Rekeying (parts of) your article
 Scanning the artwork

Queries and/or remarks

- Articles in Special Issues:** Please ensure that the words 'this issue' are added (in the list and text) to any references to other articles in this Special Issue.

<p>Uncited references: References that occur in the reference list but not in the text – please position each reference in the text or delete it from the list.</p>		
<p>Missing references: References listed below were noted in the text but are missing from the reference list – please make the list complete or remove the references from the text.</p>		
Query No.	Query / remark	Response
Q1	Please check uncited reference.	
Q2	Please update Refs. 22 and 32.	
Q3	Please check the journal name in Ref. 30.	

Thank you for your assistance

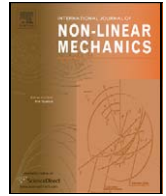
UNCORRECTED PROOF



Contents lists available at ScienceDirect

International Journal of Non-Linear Mechanics

journal homepage: www.elsevier.com/locate/nlm



1

A conditionally linearized Monte Carlo filter in non-linear structural dynamics

3 R. Sajeed, C.S. Manohar*, D. Roy

Structures Lab, Department of Civil Engineering, Indian Institute of Science, Bangalore 560012, India

ARTICLE INFO

Article history:
 Received 18 July 2008
 Received in revised form 4 March 2009
 Accepted 15 April 2009

Keywords:
 State estimation
 Non-linear dynamical systems
 Particle filters
 Ito–Taylor expansions

ABSTRACT

State and parameter estimations of non-linear dynamical systems, based on incomplete and noisy measurements, are considered using Monte Carlo simulations. Given the measurements, the proposed method obtains the marginalized posterior distribution of an appropriately chosen (ideally small) subset of the state vector using a particle filter. Samples (particles) of the marginalized states are then used to construct a family of conditionally linearized system of equations and thus obtain the posterior distribution of the states using a bank of Kalman filters. Discrete process equations for the marginalized states are derived through truncated Ito–Taylor expansions. Increased analyticity and reduced dispersion of weights computed over a smaller sample space of marginalized states are the key features of the filter that help achieve smaller sample variance of the estimates. Numerical illustrations are provided for state/parameter estimations of a Duffing oscillator and a 3-DOF non-linear oscillator. Performance of the filter in parameter estimation is also assessed using measurements obtained through experiments on simple models in the laboratory. Despite an added computational cost, the results verify that the proposed filter generally produces estimates with lower sample variance over the standard sequential importance sampling (SIS) filter.

© 2009 Published by Elsevier Ltd.

5

7 1. Introduction

9 State estimation of dynamic systems is an important problem
 11 in many engineering applications. In feedback control of dynamical
 13 systems, the states of the system need to be estimated from avail-
 15 able noisy measurements. Structural health monitoring requires the
 17 estimation of both states and parameters. Also, parameter identi-
 19 fication of non-linear vibrating systems is of fundamental impor-
 21 tance in understanding the structural behavior under extreme load-
 23 ing conditions. For linear systems under Gaussian additive noises,
 25 Kalman filter provides the optimal estimate [14]. For non-linear sys-
 27 tems, there are two main classes of methods, viz., the suboptimal
 filtering strategies such as the extended Kalman filter (EKF) or its
 variants [1,9,10,13,31] and those based on Monte Carlo (MC) sim-
 ulations, known as particle filters. The exploitation of the EKF within
 the framework of particle filters has also been explored [17]. These
 filters, referred to as Gaussian particle filters and Gaussian sum par-
 ticle filters, approximate the posterior density by a mixture of Gaus-
 sian densities obtainable from a bank of EKFs. Using a Gaussian ap-
 proximation of the states, EKF based methods aim at updating only
 the first two moments of the conditional pdf of the states and hence
 these methods may be inappropriate for highly non-linear systems.

In particle filters, the conditional pdf of the states is recursively rep-
 29 resented using a set of random particles (instantaneous realizations
 31 of states) with associated weights. Hence they are more versatile
 33 in handling system non-linearity and even non-Gaussian nature of
 35 noises. Different versions of the particle filter have been reported
 37 in the literature [6,7,8,11,12,20,23,27,33,34]. Particle filters are ex-
 tensively used in navigation and tracking applications. Their use in
 structural system identification is also reported in a few recent arti-
 cles [2,3,11,19,21,32,35].

In the identification of uncertain dynamical systems, one is
 39 also concerned about confidence levels of the estimates (typically
 41 quantified by second or higher order moments) in addition to their
 43 accuracy [15]. One important source of variability in particle filter-
 45 ing is associated with sampling fluctuations arising out of statistical
 47 nature of treatment of the filtering problem. In this context variance
 49 reduction techniques assume significance in system identification
 51 procedures. There is a general principle called Rao-Blackwellization,
 53 which aims at combining Monte Carlo simulations (particle filter)
 55 with analytic computation (Kalman filter) [20,28]. This technique is
 known to reduce the variance of the estimator and provide more
 accurate estimates than standard particle filters. An implication of
 Rao-Blackwellization is that one should carry out analytical calcula-
 tions as much as possible [20]. In order to apply Rao-Blackwellization
 in its original form, the state vector must be partitioned into two
 sets such that, given the information on one set of states, the model
 formed by the other set of states becomes linear Gaussian. How-
 ever, such a partitioning is generally not possible in the state space

* Corresponding author. Tel.: +91 80 22933121; fax: +91 80 23600404.
 E-mail addresses: sajeed@civil.iisc.ernet.in, manohar@civil.iisc.ernet.in (C.S. Manohar), royd@civil.iisc.ernet.in

1 model of a structural system as different parts are coupled with each
 2 other. Recently, the authors have proposed a novel variation of the
 3 Rao-Blackwellized particle filter (RBPf) for a class of non-linear sys-
 4 tems, in which the structure is divided into linear and non-linear
 5 substructures [32]. But, as the number of substructures increases,
 6 the procedure becomes complex. In this study, we propose a method
 7 in which a particle filter is first used to estimate a subset of the
 8 states typically associated with the non-linear terms of the process
 9 and measurement drift fields. Conditioned on the marginalized par-
 10 ticles, a bank of Kalman filters is then employed to estimate the full
 11 state vector and thus obtain the particles from the posterior density
 12 within the framework of Monte Carlo simulations. If the drift non-
 13 linearity is localized, the information of a few states provided by the
 14 particle filter transforms the given model to a family of condition-
 15 ally linear systems. The focus of the study is on assessing the effect
 16 of the increased analyticity in the filtering algorithm on the accu-
 17 racy and sampling fluctuations. Numerical illustrations on state and
 18 parameter estimations of a 1-DOF Duffing oscillator and a 3-DOF os-
 19 cillator are provided. The performance of the filter in parameter es-
 20 timation conditioned on measurements via experiments on models
 21 in the laboratory is also reported. Numerical and experiment-aided
 22 results clearly indicate the superiority of the proposed filter over
 23 the standard sequential importance sampling (SIS) filter in state and
 24 parameter estimations.

25 **2. Methodology**

26 **2.1. Governing equations**

27 Consider a non-linear dynamical system given by the state space
 28 model:

29 $\dot{x} = f(x, u(t), t, \zeta(t))$ (1)

30 $x \in \mathfrak{N}^{n_x}$ represents the state vector, $u(t) \in \mathfrak{N}^m$ the vector of external
 31 loads and $\zeta(t) \in \mathfrak{N}^q$ the process noise. A general form of the mea-
 32 surement equation may be written as

33 $y = \bar{h}(x, \zeta(t))$ (2)

34 $y \in \mathfrak{N}^{n_y}$ represents the vector of measurements, $\zeta(t) \in \mathfrak{N}^q$ the mea-
 35 surement noise and \bar{h} a sufficiently smooth function of its argu-
 36 ments. We assume process and measurement noises to be additive
 37 and Gaussian. The stochastic differential equation (SDE) correspond-
 38 ing to Eq. (1) may be expressed as

39 $dx = a(x, u(t), t) dt + D dB$ (3)

40 $a(x, u(t), t) \in \mathfrak{N}^{n_x}$ represents the drift vector, $D \in \mathfrak{N}^{n_x \times q}$ the diffusion
 41 matrix and $B \in \mathfrak{N}^q$ a vector of independently evolving q standard
 42 Brownian motion processes.

43 Let $\tilde{x} \in \mathfrak{N}^{n_{\tilde{x}}}$ be a subset of x such that the non-linear (drift) terms
 44 in the process and measurement equations are non-linear in \tilde{x} alone.
 45 We assume that the non-linear terms are sufficiently smooth func-
 46 tions of x . Now, conditioned on (all finite dimensional filtrations gen-
 47 erated by) these non-linear terms up to the current instant, both the
 48 process and measurement equations may be interpreted as being
 49 conditionally linear with a jointly Gaussian distribution. Note that,
 50 by Kolmogorov's extension theorem, a suitable collection of these
 51 filtrations along with the associated finite-dimensional probability
 52 distributions adequately determines the stochastic processes gener-
 53 ated by the non-linear terms. In other words, one may approximately
 54 accomplish the required conditioning on appropriately discretized
 55 non-linear terms, consistent with the temporal discretization being
 56 employed for solving the SDEs. We denote $\{x\} = \{x\} \setminus \{\tilde{x}\}$ and write
 57 the i th component of a as

58 $a_i(x, u(t), t) = \bar{a}_i^T x + g_i(\tilde{x}, \hat{x}, t) + b_i^T u(t)$ (4)

59 $\bar{a}_i \in \mathfrak{N}^{n_x}$ and $b_i \in \mathfrak{N}^m$ are constant vectors and $g_i(\tilde{x}, \hat{x}, t)$ is a non-
 60 linear scalar function in \tilde{x} . Eq. (3) may now be expressed as

61 $dx = [Ax + \bar{B}u(t) + G(\tilde{x}, \hat{x}, t)] dt + D dB$ (5)

62 where $A = [\bar{a}_1 \ \bar{a}_2 \ \dots \ \bar{a}_{n_x}]^T \in \mathfrak{N}^{n_x \times n_x}$, $G = [g_1(\tilde{x}, \hat{x}, t) \ g_2(\tilde{x}, \hat{x}, t) \ \dots \ g_{n_x}$
 63 $(\tilde{x}, \hat{x}, t)]^T \in \mathfrak{N}^{n_x}$ and $\bar{B} = [b_1 \ b_2 \ \dots \ b_{n_x}]^T \in \mathfrak{N}^{n_x \times m}$. Let the time
 64 axis (t_0, T) be discretized as $t_0, t_1, t_2, \dots, t_{k-1}, t_k, \dots, T$ with step size
 65 $h = t_k - t_{k-1}$ being uniform. We obtain an approximate solution
 66 for the SDE (5) in the form of a discrete map via a variant of local
 67 linearization [29,30], wherein we replace $G(\tilde{x}, \hat{x}, t)$ by $G(\tilde{x}_k, \hat{x}_{k-1}, t)$
 68 over $t \in (t_{k-1}, t_k)$. The resulting solution map is given by

69 $x_k = \phi_{k-1} x_{k-1} + \Gamma_{k-1}(\hat{x}_{k-1}, \tilde{x}_k) + w_k$ (6)

70 where $\phi_{k-1} = e^{Ah}$ and $w_k = \int_{t_{k-1}}^{t_k} D e^{A(t_k-\tau)} dB(\tau) \in \mathfrak{N}^{n_x}$ is a vector of
 71 zero mean additive Gaussian noises (martingales) whose covariance
 72 matrix (Q_k) is given by

73 $Q_k = E[w_k w_k^T] = \int_{t_{k-1}}^{t_k} e^{A(t_k-\tau)} D D^T (e^{A(t_k-\tau)})^T d\tau$ (7)

74 Moreover, we have $\Gamma_{k-1}(\hat{x}_{k-1}, \tilde{x}_k) = \int_{t_{k-1}}^{t_k} e^{A(t_k-\tau)} [\bar{B}u(\tau) + G(\tilde{x}_k, \hat{x}_{k-1}, \tau)] d\tau$.
 75 Note that, within a Monte Carlo simulation, a specific realization
 76 (say the i th realization, $i \in [1, N]$) of $\Gamma_{k-1}(\hat{x}_{k-1}, \tilde{x}_k)$ is given by
 77 $\Gamma_{k-1}^{(i)} = \Gamma_{k-1}(\hat{x}_{k-1}^{(i)}, \tilde{x}_k^{(i)})$. Using Ito-Taylor expansions, a discrete
 78 model of the components of \tilde{x} (for use with the particle filter) may
 79 be obtained as

80 $\tilde{x}_k = f(x_{k-1}, \tilde{\zeta}_k)$ (8)

81 where $\tilde{\zeta}_k$ is a noise vector containing the multiple stochastic inte-
 82 grals (MSIs) that are integrals of the form $I_{ri} = \int_{t_{k-1}}^{t_k} \int_{t_{k-1}}^s dB_r(s_1) dB_i(s)$,
 83 $I_{rj} = \int_{t_{k-1}}^{t_k} \int_{t_{k-1}}^s \int_{t_{k-1}}^{s_1} dB_r(s_2) dB_j(s_1) dB_i(s)$, $I_{r0} = \int_{t_{k-1}}^{t_k} \int_{t_{k-1}}^s dB_r(s_1) ds$, etc.
 84 ($r, i, j \in [0, q]$). Here the integer subscripts indicate the indices of
 85 scalar Brownian motion components in the same order as they ap-
 86 pear within the integrands with $dB_0(t) = dt$.

87 A discrete form of the measurement Eq. (2) may be expressed as

88 $y_k = h(x_k) + v_k$ (9)

89 where $h(\cdot)$ is a linear/non-linear function of the state and $v_k \in \mathfrak{N}^{n_y}$
 90 represents the additive measurement noise. We assume that, in
 91 terms of \tilde{x}_k , Eq. (8) is expressible as

92 $y_k = h_1(\tilde{x}_k)x_k + h_2(\tilde{x}_k) + v_k$ (9)

93 for appropriately measurable and (weakly) smooth functions $h_1(\cdot)$
 94 and $h_2(\cdot)$. Note that $h_2(\tilde{x}_k)$ is a non-linear function in \tilde{x}_k and that,
 95 given \tilde{x}_k , $h_1(\tilde{x}_k)x_k$ is linear in x_k . By appropriately selecting \tilde{x}_k , it is
 96 often possible to express Eq. (8) in the form given by Eq. (9). We
 97 observe from Eqs. (6) and (9) that, given \tilde{x}_k , both the process and
 98 measurement equations are linear, an aspect that will be made use
 99 of in the state estimation.

100 **2.2. State estimation**

101 The objective of state estimation is to obtain the filtering density
 102 $p(x_k | y_{1:k})$, which represents the pdf of the discretized state vector
 103 conditioned on the observations available up to time t_k . From the
 104 filtering density one may obtain the quantities of interest such as
 105 conditional mean and conditional variance. Incorporating \tilde{x}_k , the fil-
 106 tering density may be expressed as

107 $p(x_k | y_{1:k}) = \int p(x_k | \tilde{x}_k, y_{1:k}) p(\tilde{x}_k | y_{1:k}) d\tilde{x}_k$ (10)

1 It may be noted that the transition kernel $p(x_k|\tilde{x}_k, y_{1:k})$ corresponds
 2 to a linear-Gaussian state space model for a given \tilde{x}_k and can thus be
 3 evaluated analytically using the Kalman filter. Note that $p(x_k|\tilde{x}_k, y_{1:k})$
 4 is a (weakly) Feller kernel (i.e., if $\Upsilon_1(\tilde{x})$ is a continuous, bounded
 5 function, then so is $\Upsilon_2(x)$, where $\Upsilon_2(x_k) = \int \Upsilon_1(\tilde{x}_k)p(x_k|\tilde{x}_k, y_{1:k})d\tilde{x}_k$).
 6 In the proposed method, the filtering density or more specifically
 7 the samples $\{x_k^{(i)}\}_{i=1}^N \sim p(x_k|y_{1:k})$ are recursively obtained through a
 8 Monte Carlo simulation that involves a particle filter to obtain the
 9 likelihood (Radon–Nikodym derivative) $p(\tilde{x}_k|y_{1:k})$, which is used with
 10 the Kalman transition kernel in Eq. (10). More specifically, samples
 11 $\{\tilde{x}_k^{(i)}\}_{i=1}^N \sim p(\tilde{x}_k|y_{1:k})$ are obtained using a particle filter and the en-
 12 semble of densities $\{p(x_k|\tilde{x}_k^{(i)}, y_{1:k})\}_{i=1}^N$ is obtained analytically through
 13 a bank of Kalman filters. Using Eq. (10), we finally obtain a Monte
 Carlo approximation to the filtering density as

$$15 \quad p^N(x_k|y_{1:k}) = \frac{1}{N} \sum_{i=1}^N p(x_k|\tilde{x}_k^{(i)}, y_{1:k}) \quad (11)$$

16 Since $p(x_k|\tilde{x}_k, y_{1:k})$ is (weakly) Feller and $\tilde{x}_k^{(i)}$ bounded almost surely
 17 (a.s.), one may prove that $\lim_{N \rightarrow \infty} p^N(x_k|y_{1:k}) = p(x_k|y_{1:k})$ (a.s.) [5].
 18 Thus, it turns out that the filtering density is a mixture of Gaus-
 19 sian densities and hence one can readily generate samples $\{x_k^{(i)}\}_{i=1}^N \sim$
 20 $p(x_k|y_{1:k})$ [26]. The conditional mean (\hat{x}_k) and variance (Σ_k) may be
 21 obtained as

$$22 \quad \hat{x}_k \cong \frac{1}{N} \sum_{j=1}^N x_k^{(j)} \quad (12a)$$

$$23 \quad \Sigma_k \cong \frac{1}{N} \sum_{j=1}^N (x_k^{(j)} - \hat{x}_k)(x_k^{(j)} - \hat{x}_k)^T \quad (12b)$$

24 It may be noted that it is required to find $p(y_k|\tilde{x}_k)$ in the particle
 25 filter and thus, while selecting \tilde{x} , we generally need to include all the
 26 states appearing in the observation equation. However, as is often
 27 the case, suppose that the measured vector y_k admits partitioning
 as $y_k = [\{y_k^I\}^T, \{y_k^{II}\}^T]^T$ with y_k^I and y_k^{II} given by

$$28 \quad y_k^I = f_1(\tilde{x}_k) + v_{1k} \quad (13a)$$

$$29 \quad y_k^{II} = f_2(\tilde{x}_k) + v_{2k} \quad (13b)$$

30 Recall that $\{\tilde{x}\}$ denotes the complement of \tilde{x}_k in x_k , v_{1k} and v_{2k} are
 31 the noises in the measurement subsets y_k^I and y_k^{II} , respectively. In
 32 this case, $p(\tilde{x}_k|y_{1:k}) = p(\tilde{x}_k|y_{1:k}^I)$ and thus $p(y_k|\tilde{x}_k)$ may be obtained
 33 as $p(y_k|\tilde{x}_k) = p_{v_{1k}}(y_k - f_1(\tilde{x}_k))$. Accordingly, it suffices to consider the
 34 subset of equations for y_k^I as the measurement equations within the
 35 particle filter. We provide below the algorithm for implementing the
 36 proposed filter.

- 37 1. Set $k=0$. Draw samples $\{x_0^{(i)}\}_{i=1}^N$ from the initial pdf $p(x_0)$ and set
- 38 $k=1$.
- 39 2. As y_k arrives, use the particle filter to obtain samples $\{\tilde{x}_k^{(i)}\}_{i=1}^N \sim$
- 40 $p(\tilde{x}_k|y_{1:k})$.
- 41 3. For each $\tilde{x}_k^{(i)}$, $i \in [1, N]$, obtain the density $p(x_k|\tilde{x}_k^{(i)}, y_{1:k})$ using
- 42 Kalman filter. Construct the filtering density via Eq. (11) and gener-
 43 ate samples $\{x_k^{(i)}\}_{i=1}^N \sim p(x_k|y_{1:k})$. Estimate the conditional mean
 44 and conditional variance using Eq. (12).

- 45 4. Replace k by $k+1$ and recursively use steps 2 and 3 till the terminal
 46 time is reached.

47 Thus the proposed filter estimates the states in two stages; the
 48 marginalized states (defining the localized non-linearity) are first
 49 estimated using a particle filter and then, making use of the infor-
 50 mation available on these states, the resulting conditionally linear
 51 systems are analyzed through a bank of Kalman filters. The same
 52 steps are also valid for parameter estimations, as these parameters
 53 are declared as additional states within the dynamic filtering frame-
 54 work. Unlike the Rao-Blackwellized particle filter wherein estima-
 55 tions of a few states are done using a particle filter and the remain-
 56 ing states by a bank of Kalman filters, the proposed method obtains
 57 the conditional pdf of all the states through a bank of Kalman fil-
 58 ters. Roughly speaking, since we typically have $\dim(\tilde{x}) \ll \dim(x)$ for
 59 oscillators with localized non-linearity and the fact that weights are
 60 proportional to the marginalized posterior density $p(\tilde{x}_k|y_{1:k})$, sam-
 61 ple variance due to dispersion of weights, computed over a reduced
 62 sample space containing the marginalized states, will be less for a
 63 given N . Indeed, if $\dim(\tilde{x})=0$, then we recover the analytical Kalman
 64 estimate with zero sample variance. These statements may be made
 65 mathematically more precise by defining appropriate sample vari-
 66 ances associated with the Kalman prediction and weight calculation
 67 steps followed by the use of Jensen's inequality (somewhat similar
 68 to the proof of Theorem 4 in [4]). This exercise will be taken up in a
 69 future study.

3. Numerical implementation of the filter

70 The central idea of the proposed method is the conditional lin-
 71 earization of the process/observation equations so that analyticity of
 72 the Kalman filter can be exploited in the state estimation procedure.
 73 The process and measurement equations need to be expressed in a
 74 form consistent with Eqs. (6) and (8). Further illustration is facili-
 75 tated by considering specific examples and we presently consider
 76 a 1-DOF Duffing oscillator and a 3-DOF spring mass oscillator with
 77 localized non-linearity.

78 The governing SDEs of the Duffing oscillator, subjected to support
 79 motion and additive white noise excitation, may be expressed in the
 80 following incremental form:

$$81 \quad \left. \begin{aligned} dx_1 &= x_2 dt \\ dx_2 &= \left\{ \frac{1}{m} [\alpha x_1 + \beta x_1^3 + c x_2] - \ddot{x}_g \right\} dt + \sigma_d dB_1 \end{aligned} \right\} \quad (14)$$

82 with initial conditions $x_i(0)=x_{i0}$, $i \in [1, 2]$. Here α , β and c represent
 83 the system parameters and x_g represents the support motion. σ_d is
 84 the additive diffusion coefficient representing the process noise and
 85 dB_1 increments of a standard Brownian motion process. Eq. (14) is
 86 the process equation. The discrete form of the measurement model
 87 is assumed to be

$$88 \quad y_k = x_{1k} + v_k \quad (15)$$

89 where v_k denotes the measurement noise. It may be observed that
 90 Eq. (14) is conditionally linear provided that it is appropriately con-
 91 ditioned on x_1^2 , the non-linear term. In the proposed procedure, we
 92 declare $\tilde{x} = x_1$ (also denoted as \tilde{x}_1) and, for subsequent linearization
 93 of the process equation, we must estimate \tilde{x}_1 through particle filter-
 94 ing. The linearized process equation (conditioned on \tilde{x}_1^2) may then
 95 be expressed as

$$96 \quad \left\{ \begin{aligned} dx_1 \\ dx_2 \end{aligned} \right\} = \left[\begin{array}{cc} 0 & 1 \\ -\frac{\alpha}{m} & -\frac{c}{m} \end{array} \right] \left\{ \begin{aligned} x_1 \\ x_2 \end{aligned} \right\} dt + \left\{ \begin{array}{c} 0 \\ -\frac{\beta}{m} \tilde{x}_1^2 - \ddot{x}_g \end{array} \right\} dt + \left\{ \begin{array}{c} 0 \\ \sigma_d \end{array} \right\} dB_1 \quad (16)$$

97 Eq. (16) may be converted to a discrete form (as in Eq. (7)) using a
 98 stochastic Taylor (Ito–Taylor) expansion. Note that the observation
 99 Eq. (15) in the present example is already linear. Details of Ito–Taylor
 100

expansions and related concepts in stochastic calculus may be found in [16,21,24,25]. Using an explicit and truncated Ito–Taylor expansion, the discrete map for \tilde{x}_1 over the interval (t_{k-1}, t_k) (with a uniform step-size $h = t_k - t_{k-1}$) may be written as

$$\tilde{x}_{1k} = x_{1,k-1} + x_{2,k-1}h + a_{2,k-1} \frac{h^2}{2} - \frac{1}{m}(\alpha x_{2,k-1} + 3\beta x_{1,k-1}^2 x_{2,k-1} + ca_{2,k-1}) \frac{h^3}{6} + \sigma_d I_{10} - \frac{c}{m} \sigma_d I_{100} \quad (17)$$

$$\begin{Bmatrix} dx_1 \\ dx_2 \\ dx_3 \\ dx_4 \\ dx_5 \\ dx_6 \end{Bmatrix} = \begin{bmatrix} 0 & 0 & 0 & 1 & 0 & 0 \\ 0 & 0 & 0 & 0 & 1 & 0 \\ 0 & 0 & 0 & 0 & 0 & 1 \\ -\frac{(k_1+k_2)}{m_1} & \frac{k_2}{m_1} & 0 & \frac{-(c_1+c_2)}{m_1} & \frac{c_2}{m_1} & 0 \\ \frac{k_2}{m_2} & \frac{-(k_2+k_3)}{m_2} & \frac{k_3}{m_2} & \frac{c_2}{m_2} & \frac{-(c_2+c_3)}{m_2} & \frac{c_3}{m_2} \\ 0 & \frac{k_3}{m_3} & \frac{-k_3}{m_3} & 0 & \frac{c_3}{m_3} & \frac{-c_3}{m_3} \end{bmatrix} \begin{Bmatrix} x_1 \\ x_2 \\ x_3 \\ x_4 \\ x_5 \\ x_6 \end{Bmatrix} dt + \begin{Bmatrix} 0 \\ 0 \\ 0 \\ -\frac{1}{m_1} [qk_b \tilde{x}_1 - \mu_1(1 - \tilde{x}_1^2) \tilde{x}_4 + \mu_2 \tanh(\kappa \tilde{x}_4)] \\ 0 \\ 0 \\ 0 \end{Bmatrix} dt + \begin{bmatrix} 0 & 0 & 0 \\ 0 & 0 & 0 \\ 0 & 0 & 0 \\ \sigma_1 & 0 & 0 \\ 0 & \sigma_2 & 0 \\ 0 & 0 & \sigma_3 \end{bmatrix} \begin{Bmatrix} dB_1 \\ dB_2 \\ dB_3 \end{Bmatrix} \quad (23)$$

Eq. (17) serves as the process equation for the particle filter and the observation equation is given by Eq. (15) with x_{1k} replaced by \tilde{x}_{1k} .

The 3-DOF oscillator with localized non-linearity is shown in Fig. 1(a). The first spring is assumed to have a bilinear force-displacement relation (Fig. 1b). The force resisted by the first spring is thus given by

$$f_s(x_1) = k_1 x_1 \quad \text{if } x_1 \leq 0 \\ = (k_1 + k_b) x_1 \quad \text{if } x_1 > 0 \quad (18)$$

A more general form of the above equation may be written as

$$f_s(x_1) = p k_1 x_1 + q(k_1 + k_b) x_1 \quad (19)$$

p and q are presently given by $p = 1, q = 0$ if $x \leq 0$ and $p = 0, q = 1$ otherwise. The damping force in the first segment (acting to the left of first mass point) is assumed to be of the form $c_1 \dot{x}_1 - \mu_1(1 - x_1^2) \dot{x}_1 + \mu_2 \text{sgn}(\dot{x}_1)$. In order to conform to the smoothness requirement of the truncated Ito–Taylor expansion, the discontinuous signum function is approximated as $\tanh(\kappa \dot{x}_1)$, where $\kappa > 0$. Note that $\tanh(\kappa \dot{x}_1) \rightarrow \text{sgn}(\dot{x}_1)$ as $\kappa \rightarrow \infty$. Indeed, a continuous approximation of the signum function is achievable in multiple ways. For instance $2/\pi \tan^{-1}(\gamma \dot{x})$ may also be used to approximate $\text{sgn}(\dot{x})$ ($2/\pi \tan^{-1}(\gamma \dot{x}) \rightarrow \text{sgn}(\dot{x})$ almost surely as $\gamma \rightarrow \infty$).

The governing SDEs of the 3-DOF system in incremental form may be expressed as

$$\left. \begin{aligned} dx_1 &= x_4 dt; & dx_2 &= x_5 dt; & dx_3 &= x_6 dt; \\ dx_4 &= a_4 dt + \sigma_1 dB_1; & dx_5 &= a_5 dt + \sigma_2 dB_2; & dx_6 &= a_6 dt + \sigma_3 dB_3 \end{aligned} \right\} \quad (20)$$

with initial conditions $x_i(0) = x_{i0}, i \in [1, 6]$. σ_1, σ_2 and σ_3 are the additive diffusion coefficients representing the process noise. The drift coefficient functions are given by

$$\left. \begin{aligned} a_4 &= -\frac{1}{m_1} [p k_1 x_1 + q(k_1 + k_b) x_1 - \mu_1(1 - x_1^2) x_4 + \mu_2 \tanh(\kappa x_4) \\ &\quad + c_1 x_4 + k_2(x_1 - x_2) + c_2(x_4 - x_5)] - \ddot{x}_g \\ a_5 &= -\frac{1}{m_2} [k_2(x_2 - x_1) + k_3(x_2 - x_3) + c_2(x_5 - x_4) + c_3(x_5 - x_6)] - \ddot{x}_g \\ a_6 &= -\frac{1}{m_2} [k_3(x_3 - x_2) + c_3(x_6 - x_5)] - \ddot{x}_g \end{aligned} \right\} \quad (21)$$

The force transmitted to the support is assumed to be measured. Thus the observation equation is also non-linear in this case. A discrete form of the measurement equation is given by

$$y_k = p k_1 x_{1k} + q(k_1 + k_b) x_{1k} + c_1 x_{4k} - \mu_1(1 - x_{1k}^2) x_{4k} + \mu_2 \tanh(\kappa x_{4k}) + v_k \quad (22)$$

where v_k represents the measurement noise. Given x_1 and x_4 , the process equation (Eq. (20)) and the measurement equation (Eq. (22)) are linear. Thus one may declare $\tilde{x} = \{x_1; x_4\}^T$, which are the states to be estimated using the particle filter. Given \tilde{x} , the process Eq. (20) may be expressed in a conditionally linearized form as

The observation equation (Eq. (22)) may be expressed in a linear form as

$$y_k = H_k x_k + \mu_2 \tanh(\kappa \tilde{x}_{4k}) + v_k \quad (24)$$

$$H_k = [k_1 + q k_b \quad 0 \quad 0 \quad c_1 - \mu_1(1 - \tilde{x}_{1k}^2) \quad 0 \quad 0] \quad \text{and} \\ x_k = [x_{1k} \quad x_{2k} \quad x_{3k} \quad x_{5k} \quad x_{6k}]^T$$

Note that Eq. (24) is in the form given by Eq. (9). Using truncated Ito–Taylor expansions, discrete maps of respective local orders $O(h^{2.5})$ and $O(h^{1.5})$ for \tilde{x}_1 and \tilde{x}_4 over (t_{k-1}, t_k) are obtainable as

$$\begin{aligned} \tilde{x}_{1k} &= x_{1,k-1} + x_{4,k-1}h + a_{4,k-1} \frac{h^2}{2} - \frac{1}{m_1} \{ [p k_1 + q(k_1 + k_b)] x_{4,k-1} \\ &\quad - \mu_1(1 - x_{1,k-1}^2) a_{4,k-1} + 2\mu_1 x_{1,k-1} x_{4,k-1}^2 \\ &\quad + \mu_2 \kappa [1 - \tanh^2(\kappa x_{4,k-1})] a_{4,k-1} \\ &\quad + c_1 a_{4,k-1} + k_2(x_{4,k-1} - x_{5,k-1}) \} h^3/6 \\ &\quad + \sigma_1 I_{10} - \frac{1}{m_1} [-\mu_1(1 - x_{1,k-1}^2) \\ &\quad + \mu_2 \kappa [1 - \tanh^2(\kappa x_{4,k-1})] + c_1] \sigma_1 I_{100} \\ &\quad - \frac{c_2}{m_1} (\sigma_1 I_{100} - \sigma_2 I_{200}) \end{aligned} \quad (25a)$$

$$\begin{aligned} \tilde{x}_{4k} &= x_{4,k-1} + a_{4,k-1}h - \frac{1}{m_1} \{ [p k_1 + q(k_1 + k_b)] x_{4,k-1} - \mu_1(1 - x_{1,k-1}^2) \\ &\quad \times a_{4,k-1} + 2\mu_1 x_{1,k-1} x_{4,k-1}^2 \\ &\quad + \mu_2 \kappa [1 - \tanh^2(\kappa x_{4,k-1})] a_{4,k-1} \\ &\quad + c_1 a_{4,k-1} + k_2(x_{4,k-1} - x_{5,k-1}) \} h^2/2 \\ &\quad + \sigma_1 I_1 - \frac{1}{m_1} [-\mu_1(1 - x_{1,k-1}^2) \\ &\quad + \mu_2 \kappa (1 - \tanh^2(\kappa x_{4,k-1})) + c_1] \sigma_1 I_{10} \\ &\quad - \frac{c_2}{m_1} (\sigma_1 I_{10} - \sigma_2 I_{20}) \end{aligned} \quad (25b)$$

While these equations constitute the process equation for the particle filter, the observation equation is given by Eq. (22) with x_{1k} and x_{4k} replaced by \tilde{x}_{1k} and \tilde{x}_{4k} , respectively. The quantities I_r, I_{r0}

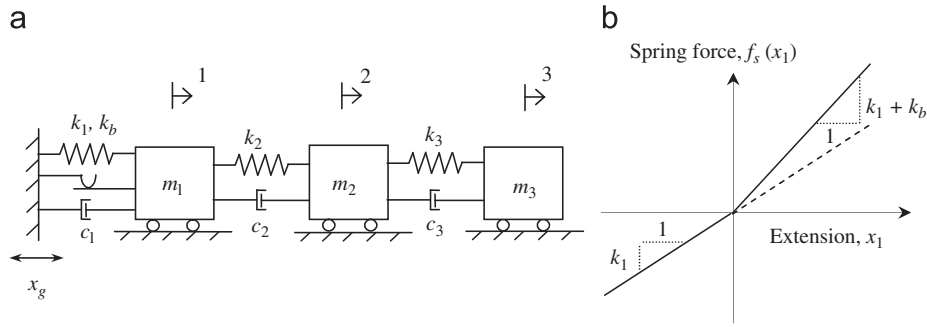


Fig. 1. (a) The 3-DOF system with localized non-linearity and (b) force–displacement relation of the first spring.

1 and I_{r00} ($r = 1, 2$) used in Eqs. (17) and (25) are MSIs given by 37

$$\begin{aligned}
 I_1 &= \int_{t_{k-1}}^{t_k} dB_1, \quad I_{r0} = \int_{t_{k-1}}^{t_k} \int_{t_{k-1}}^s dB_r ds_1 \quad \text{and} \\
 I_{r00} &= \int_{t_{k-1}}^{t_k} \int_{t_{k-1}}^s \int_{t_{k-1}}^{s_1} dB_r ds_1 ds_2 \quad (26)
 \end{aligned}$$

3 These MSIs are zero mean, normal random variables. Details of evalu- 41
 5 ating these MSIs may be found in [16]. The approximating the 43
 7 signum function as mentioned above allows the vector field to be 45
 9 adequately differentiable and this helps to obtain the discrete maps 47
 11 of the SDEs in a weak form. To assess the error introduced due to 49
 13 this approximation, it may be necessary to obtain the solution of the 51
 15 SDEs in the strong form. This requires the detection of the event $\chi=0$ 53
 17 (where the signum function fails to be differentiable). However, an 55
 19 accurate detection of such events in the solutions of SDEs is still an 57
 open research problem and is not attempted in the present study.

13 To estimate the parameters, within the framework of dynamic 51
 15 state estimation, one needs to extend the state vector by declaring 53
 17 the parameters as additional state variables. For the 3-DOF oscillator, 55
 19 we consider the estimations of k_b , μ_1 and μ_2 , the parameters that 57
 account for the non-linearity in the model. The governing SDEs of 59
 the estimation problem in incremental form (after declaring these 61
 parameters as additional states— k_b , μ_1 and μ_2 declared as x_7, x_8 , and 63
 x_9 , respectively) may be written as 65

$$\left. \begin{aligned}
 dx_1 &= x_4 dt; \quad dx_2 = x_5 dt; \quad dx_3 = x_6 dt \\
 dx_4 &= a_4 dt + \sigma_1 dB_1; \quad dx_5 = a_5 dt + \sigma_2 dB_2; \quad dx_6 = a_6 dt + \sigma_3 dB_3 \\
 dx_7 &= \sigma_k dB_4; \quad dx_8 = \sigma_{\mu_1} dB_5; \quad dx_9 = \sigma_{\mu_2} dB_6
 \end{aligned} \right\} \quad (27)$$

Here the drift coefficient function a_4 is given by

$$\begin{aligned}
 a_4 &= -\frac{1}{m_1} [pk_1 x_1 + q(k_1 + x_7)x_1 - x_8(1 - x_1^2)x_4 \\
 &\quad + x_9 \tanh(\kappa x_4) + c_1 x_4 + k_2(x_1 - x_2) + c_2(x_4 - x_5)] - \ddot{x}_g \quad (28)
 \end{aligned}$$

25 The coefficients a_5 and a_6 are the same as given in Eq. (21). σ_k , σ_{μ_1} 69
 27 and σ_{μ_2} represent the assumed diffusion coefficients in the SDEs 71
 29 for the parameter states x_7, x_8 and x_9 , respectively. As in the state 73
 estimation problem, the force transmitted to the support is assumed 75
 to be measured and hence the discrete observation equation takes 77
 the form 79

$$\begin{aligned}
 y_k &= pk_1 x_{1k} + q(k_1 + x_{7k})x_{1k} + c_1 x_{4k} - x_{8k}(1 - x_{1k}^2)x_{4k} \\
 &\quad + x_{9k} \tanh(\kappa x_{4k}) + v_k \quad (29)
 \end{aligned}$$

31 where v_k represents the measurement noise.

33 Given the states x_1, x_4, x_7, x_8 and x_9 , the process equation (27) and 81
 35 the observation equation (29) are linear. Thus \tilde{x} —the states to be esti- 83
 mated using the particle filter—is identified as $\tilde{x} = [x_1; x_4; x_7; x_8; x_9]$.
 The linearized process and the observation equations, conditioned
 on \tilde{x} , may now be readily expressed in the form of Eqs. (6) and

(9). Using truncated Ito–Taylor expansions, the discrete maps of the
 components of \tilde{x} (i.e., $\tilde{x}_1, \tilde{x}_4, \tilde{x}_7, \tilde{x}_8$ and \tilde{x}_9) over the interval $(t_{k-1}, t_k]$
 may also be obtained. 39

3.1. Numerical results

41 We now employ the proposed methodology for state and param- 41
 43 eter estimations of the Duffing and the 3-DOF oscillators. While we 43
 45 report results on state estimations of both the oscillators, we pro- 45
 47 vide results on parameter estimations of the 3-DOF oscillator only. 47
 49 In both state and parameter estimation problems, we use an SIS fil- 49
 51 ter for comparisons with results via the present filter. In parameter 51
 53 estimation problems, the unknown system parameters are treated 53
 55 as additional state variables. Discrete maps of system states, which 55
 57 serve as the process equations for the SIS filter, are obtained using 57
 truncated Ito–Taylor expansions. Details of the SIS filter are avail- 59
 61 able in [6–8,21] and skipped here for conciseness. Within the present 61
 63 filtering algorithm, we consistently use a bootstrap filter for esti- 63
 65 mating the marginalized states. All such comparisons with the SIS 65
 67 filter are reported using the same initial pdfs of all states, same pro- 67
 69 cess/measurement noise intensities and the same ensemble size. To 69
 71 study the effect of sampling fluctuations, 100 independent Monte 71
 73 Carlo runs are performed. 73
 75

75 The parameter values assumed for the Duffing oscillator are: 75
 77 $m = 1$ kg, $\alpha = 10$ N/m, $\beta = 50000$ N/m³ and $c = 0.5$ N s/m. For the 77
 79 3-DOF oscillator, the assumed parameter values are: $m_1 = m_2 = m_3 =$ 79
 81 10 kg, $k_1 = k_2 = k_3 = 3000$ N/m, $k_b = 750$ N/m, $c_1 = c_2 = c_3 = 5$ N s/m, 81
 83 $\mu_1 = 40$ N s/m³ and $\mu_2 = 5$ N. The value of κ used in the present work 83
 is 10^4 (as a quick numerical study has confirmed that a further in-
 crease in κ does not significantly change the results). All other sys-
 tem parameters are chosen arbitrarily in the present study. In state
 estimation problems, the support motion is assumed to be harmonic,
 i.e., $x_g(t) = x_{g0} \sin(\lambda t)$. The parameters x_{g0} and λ are taken as 0.03 m
 and 4 rad/s, respectively, for the Duffing oscillator. Note that the
 frequency of the support motion is close to the natural frequency
 of the oscillator without the cubic term. The natural frequencies of
 the linear model (again obtained by removing the non-linear terms)
 associated with the 3-DOF oscillator are found to be 7.7, 21.6 and
 31.2 rad/s. The support motion parameters of the 3-DOF oscillator
 are taken as $x_{g0} = 0.01$ m and $\lambda = 7$ rad/s. The process noise param-
 eter (σ_d) for the Duffing oscillator is assumed as $0.05|\ddot{x}_g|_{\max}$, where
 $|\ddot{x}_g|_{\max}$ is the maximum value of the realization of $|\ddot{x}_g(t)|$ over the
 time interval of interest. For the 3-DOF oscillator, process noise pa-
 rameters (σ_1, σ_2 and σ_3) are uniformly taken to be $0.01|\ddot{x}_g|_{\max}$. While
 the measurement equation for the Duffing oscillator is obtained by
 assuming the displacement to have been measured, the support re-
 action constitutes the measurement for the 3-DOF oscillator. In the
 numerical study, for the purpose of illustration, the time histories
 of measurements are generated synthetically. (The case of experi-

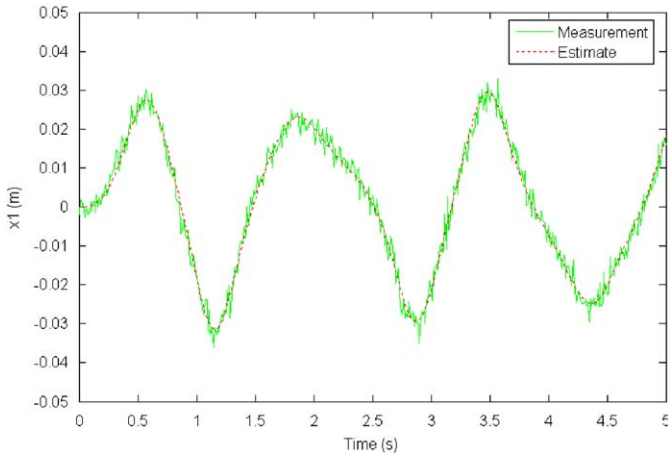


Fig. 2. State estimation of the Duffing oscillator using the proposed filter.

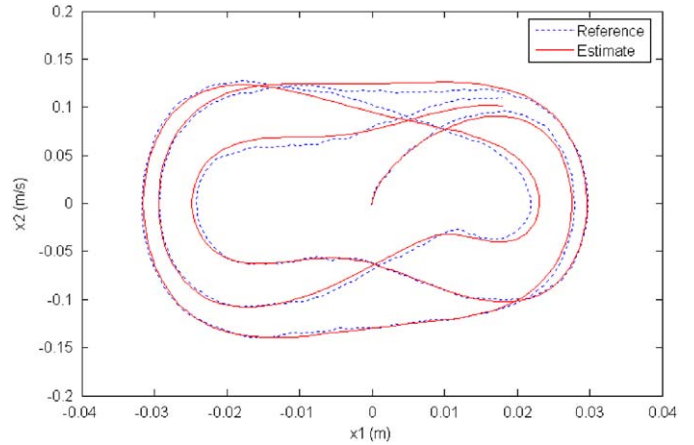


Fig. 3. State estimation of the Duffing oscillator—phase plane plot.

mentally obtained data is considered later in the paper.) For both the oscillators, the standard deviation of the measurement noise is assumed as 7.5% of the maximum absolute value of the measured quantity. A uniform step size $h = 0.01$ s is used for both the systems. The ensemble sizes used are $N = 50$ and 250 , respectively, for the Duffing and the 3-DOF systems. Both the oscillators are assumed to start from rest and the initial conditions are treated as deterministic.

In the parameter estimation problem, we consider the estimations of k_b , μ_1 and μ_2 of the 3-DOF system. The system parameters are assumed to be the same as those used in the state estimation problem. Accordingly, the reference values of the parameters to be estimated are given by $k_b^* = 750$ N/m, $\mu_1^* = 40$ N s/m³ and $\mu_2^* = 5$ N. The support motion is assumed to be a realization of the stochastic process $x_g(t) = \sum_{i=1}^n r_i \sin(\omega_i t + \theta_i)$, where r_i , ω_i and θ_i are independent random variables. While r_i is assumed to be uniformly distributed in $[-0.005, 0.005]$ m, ω_i and θ_i are assumed to be uniformly distributed in $[5, 35]$ rad/s and $[0, 90]^\circ$, respectively. Value of n is taken as 10. The initial pdf of x_7 (i.e., k_b) is assumed to be its given by its reference value times a uniformly distributed random variable in $[0.5, 1.2]$. Similarly the initial pdfs of x_8 and x_9 (i.e., μ_1 and μ_2 , respectively) are given by their respective reference values times (independently generated) uniformly distributed random variables in $[0.8, 1.5]$. We note that the deviation of the mean of the initial pdf from the true value is 15% for all parameter states. Diffusion coefficients associated with the parameter states are assumed as 10% of their reference values. The process and measurement noise parameters are taken to be the same as those used in the state estimation problem. A step size $h = 0.01$ s and an ensemble size of $N = 1000$ are uniformly used.

Results of the state estimation of the Duffing oscillator are shown in Figs. 2–7. Fig. 2 shows the measurement and one specific realization of the estimate using the proposed filter. A good convergence of the mean is observed. The phase plot is shown in Fig. 3. One trajectory amongst the ensemble of solutions of the SDE is used for generating the measurement and is taken as the so called ‘reference’ trajectory (note that this is only possible in numerical experiments involving artificial generations of measured signals). A reasonably good correspondence of the estimated trajectory with its reference is observable from Fig. 3. In order to obtain a measure of sampling fluctuations in the estimation process, 100 independent MC simulations are performed. Cumulative sampling variances of the estimated states are shown in Fig. 4. The cumulative sampling variance of the estimate of the i th state is obtained as $\text{cum.var}(E[x_i(t)]) = \int_0^t \text{var}(E[x_i(s)]) ds$. A significant reduction in the cumulative variance of the states is observable through the proposed filter. Root mean square errors (RMSEs) in the estimated states from their references

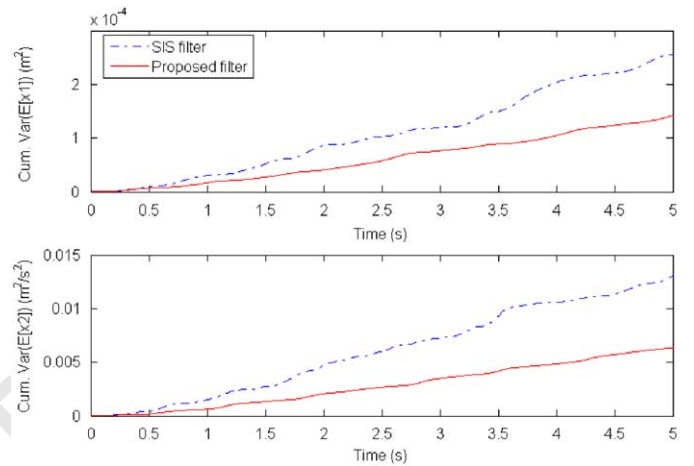


Fig. 4. State estimation of the Duffing oscillator—cumulative variance of the estimated states.

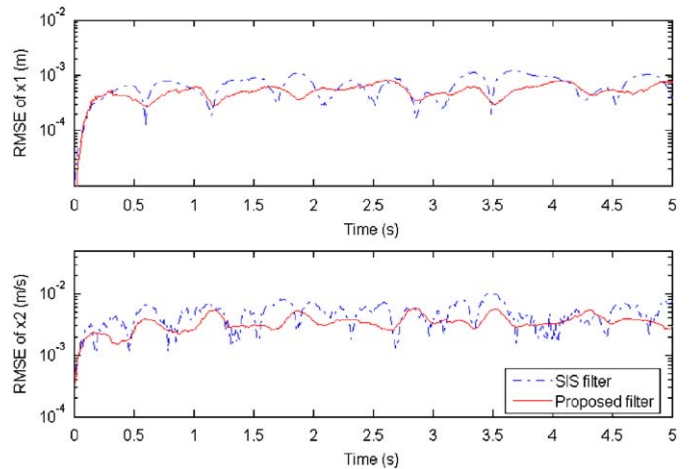


Fig. 5. State estimation of the Duffing oscillator—RMSE of the estimated states.

are shown in Fig. 5. The error in estimating the i th state is evaluated as $e_i(t) = x_{i,\text{reference}}(t) - \hat{x}_i(t)$, where \hat{x}_i is the estimated state. Compared with the SIS filter, a marginal reduction in the variances of estimated states and RMSEs could be seen in state estimations via the

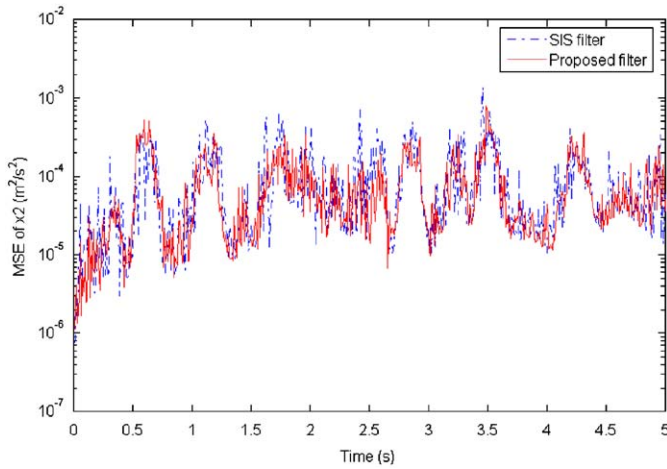


Fig. 6. State estimation of the Duffing oscillator—MSE (with reference to the solution trajectories of the system SDEs), in one of the MC runs.

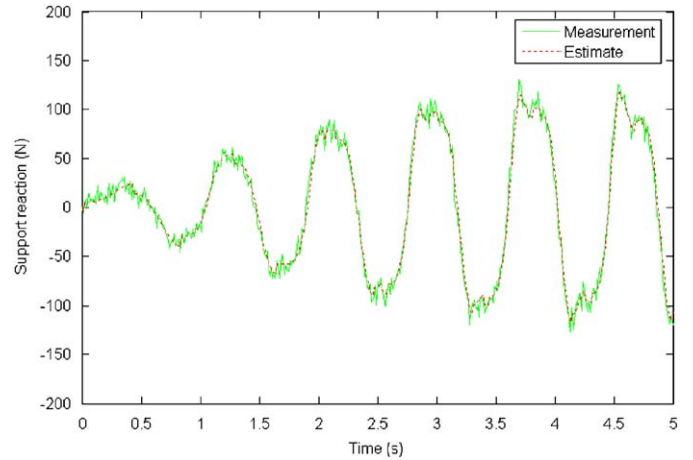


Fig. 8. State estimation of the 3-DOF oscillator using the proposed filter.

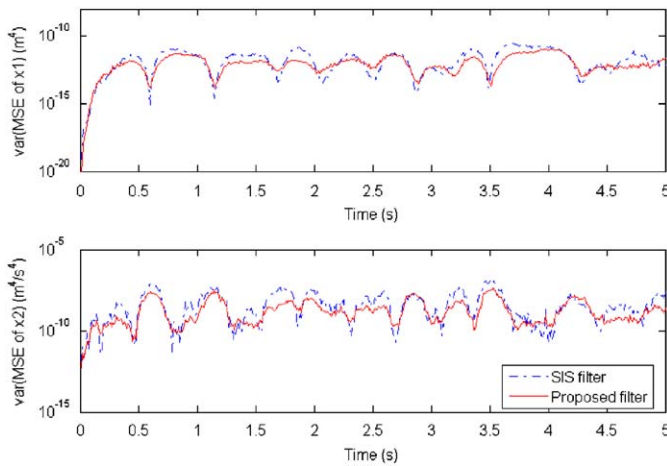


Fig. 7. State estimation of the Duffing oscillator—variance of the MSE (with reference to the solution trajectories of the system SDEs).

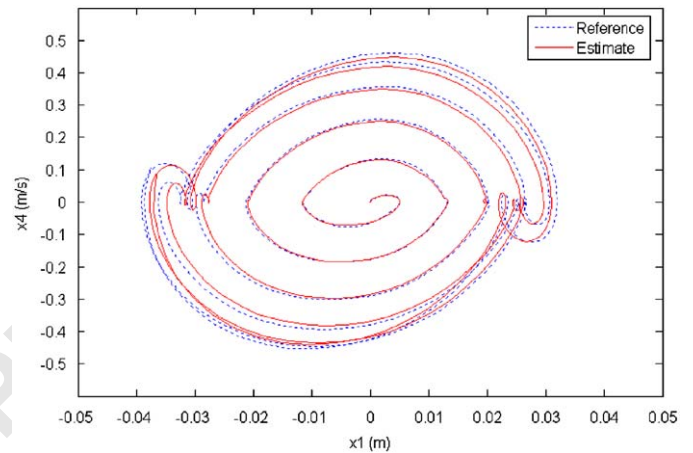


Fig. 9. State estimation of the 3-DOF oscillator—phase plane plot.

1 proposed filter. In the context practical applications, the so called
 3 reference trajectories are not available and hence the RMSE calculation
 5 as mentioned is not feasible. Nevertheless, the availability of the
 7 analytical model of the structure, built into the process equations,
 9 makes it possible to generate any number of realizations of the
 11 solution of the associated SDEs. Consequently we define the estimation
 13 error in the i th state as $\tilde{e}_i^{(j)}(t) = x_i(t, \omega_j) - \hat{x}_i(t)$, where $x_i(t, \omega_j)$ is the
 15 j -th realization of the solution of the process SDEs. Thus, the MSE
 17 in one MC run may be computed as $\sum_{j=1}^N [\tilde{e}_i^{(j)}(t)]^2$ with N being the
 19 number of particles. Fig. 6 shows the MSE in the estimate of x_2
 21 in one of the MC runs. The sample variance of the MSE, over 100 MC
 runs, is shown in Fig. 7. Here again, the robustness and accuracy of
 the proposed filter is observable. Figs. 8–14 show results on state
 estimations of the 3-DOF oscillator. Fig. 8 shows the measured support
 reaction and its estimate using the proposed filter. The phase plane
 plot is shown in Fig. 9. A fairly good convergence of the estimated
 trajectory may be observed. Fig. 10 shows the cumulative variance
 of the estimated velocity states (x_4 , x_5 and x_6) over 100 MC
 simulations. Substantial reductions in variance is visible in the
 estimated states through the proposed filter vis-à-vis the results
 obtained by the SIS filter. The MSE of the estimated states, as
 defined above, in one of the MC runs is shown in Fig. 11. A
 superior performance of

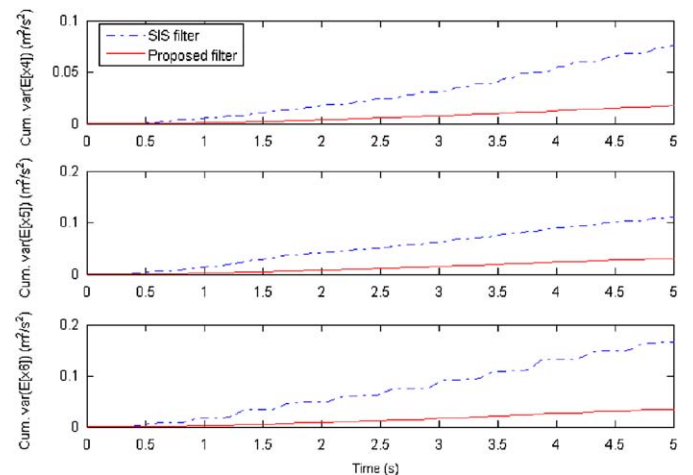


Fig. 10. State estimation of the 3-DOF oscillator—cumulative variance of the estimated velocity states.

the proposed filter over the SIS filter is evidenced from both the
 figures. For both state and parameter estimation problems of the 3-DOF
 oscillator, we mainly use $\tanh(\kappa\hat{x})$ to approximate the signum func-

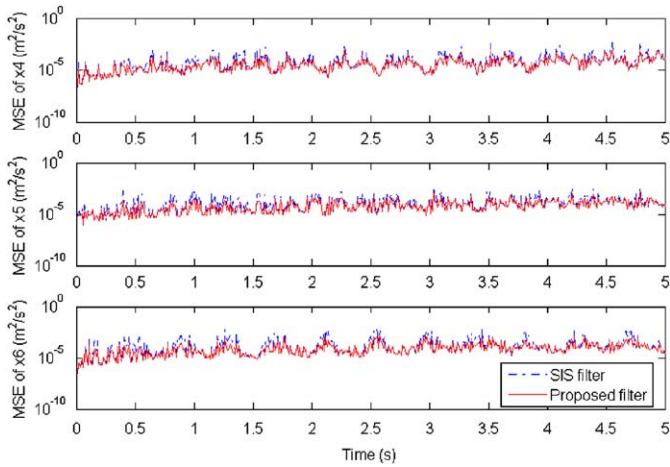


Fig. 11. State estimation of the 3-DOF oscillator—MSE (with reference to the solution trajectory of the SDE), in one of the MC runs.

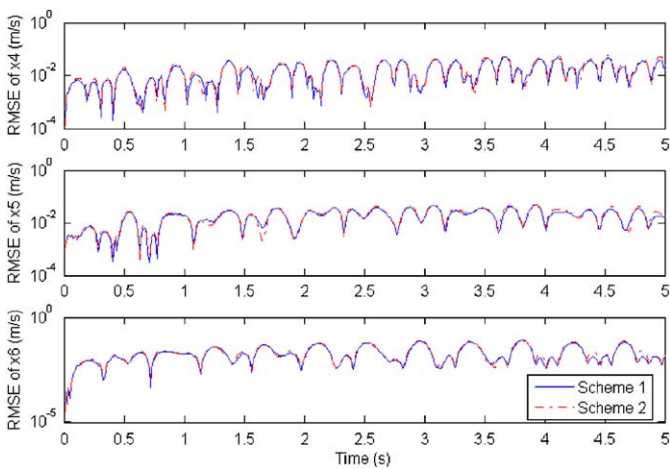


Fig. 12. State estimation of the 3-DOF oscillator using the proposed filter—RMSE of the estimated states using two different approximations of the signum function. (Scheme 1 refers to approximation of $\text{sgn}(x)$ as $\tanh(\kappa x)$ and Scheme 2 refers to approximation of $\text{sgn}(x)$ as $(2/\pi)\tan^{-1}(\gamma x)$.)

tion. However, as mentioned in the previous section, signum function can also be approximated as $2/\pi \tan^{-1}(\gamma x)$. It will be interesting to compare the error in state estimation using these two schemes of approximations for the same values of κ and γ ($\kappa = \gamma = 10^4$). Fig. 12 shows a comparison of the RMSE of the estimated states (over 100 independent MC simulations) of the 3-DOF oscillator using these two schemes of approximations of the signum function. We observe that both the schemes lead to almost identical RMSEs.

The results of parameter estimation of the 3-DOF oscillator are shown in Figs. 13 and 14. Mean of the estimated parameters, over 100 MC runs, is shown in Fig. 13. One realization (time history) of the estimate in one of the MC runs) of the estimated parameters is also shown along with the mean of the estimated parameters. Fig. 14 shows the cumulative variance of the estimated parameters in 100 MC runs. In estimating the mean of the stiffness parameter k_b , performance of both the filters is almost identical. However, in the estimation of the damping parameter μ_1 , the mean estimate using the proposed filter shows better convergence to its reference value. The mean estimate of the Coulomb damping parameter (μ_2) converges to a slightly higher value compared to its reference value, using both the filters. A single realization of the estimate of μ_2 was

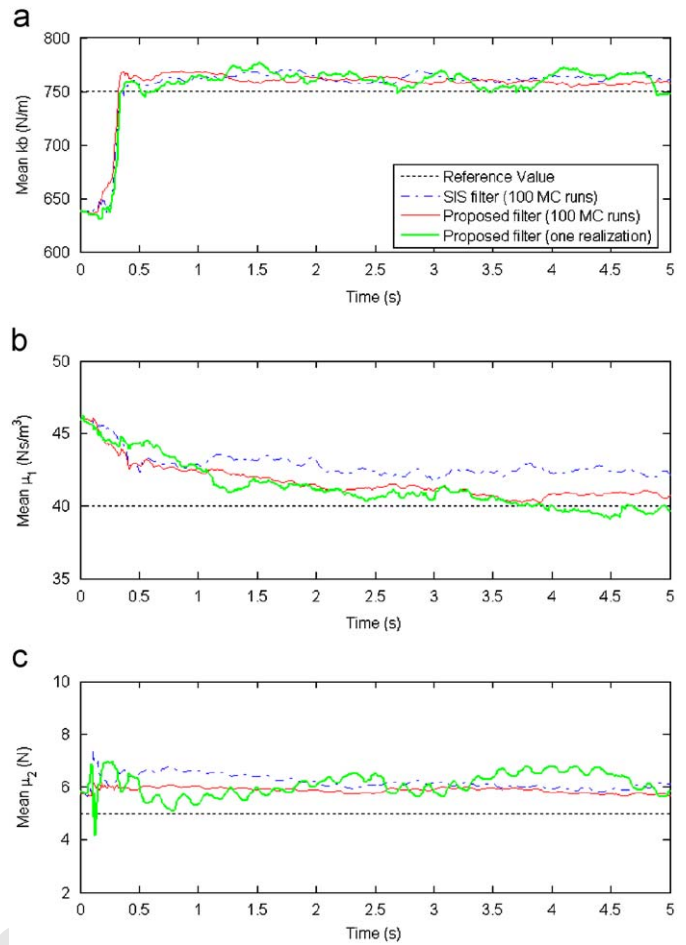


Fig. 13. Parameter estimation of the 3-DOF oscillator: (a) estimate of mean of k_b ; (b) estimate of mean of μ_1 and (c) estimate of mean of μ_2 .

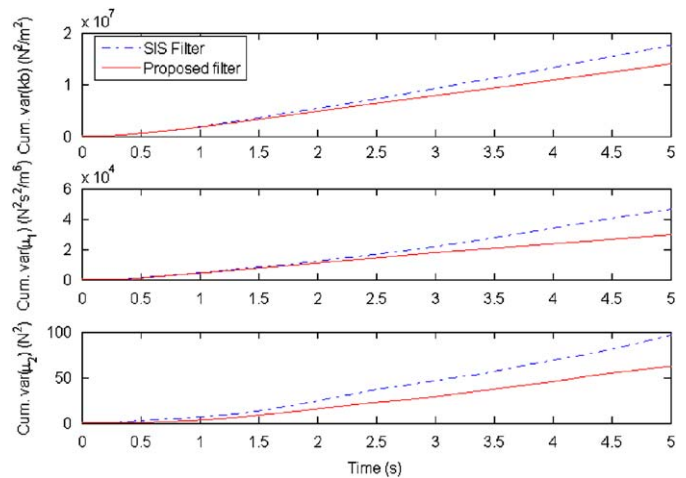


Fig. 14. Parameter estimation of the 3-DOF oscillator—cumulative sample variance of the estimated parameters.

found to be oscillatory and the convergence was found to be poor. Nevertheless, compared to the estimates using the SIS filter, mean parameter estimates using the proposed filter are generally closer to their respective reference values. The fact that estimates do not converge exactly to the reference values is only natural because of

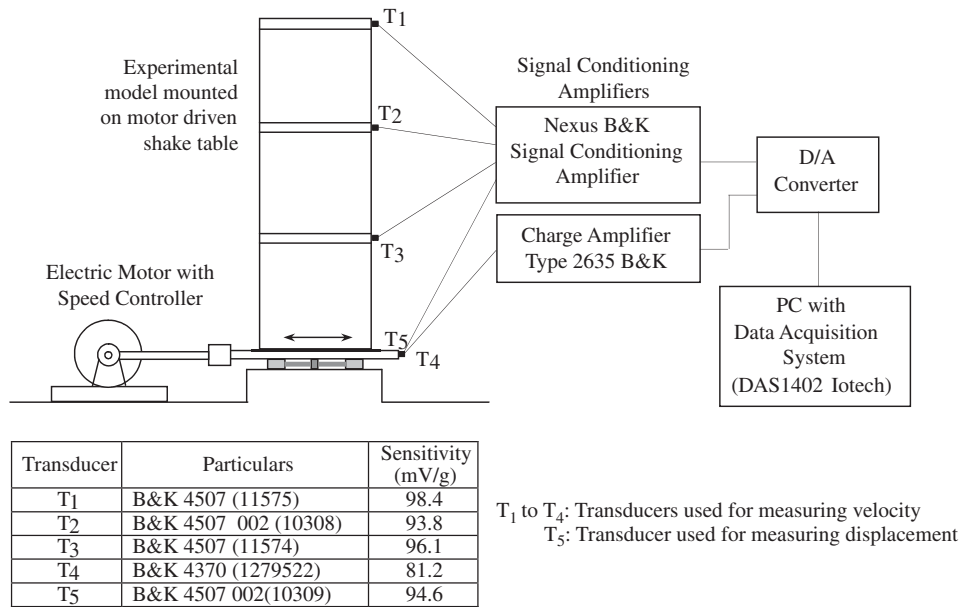


Fig. 15. Schematic diagram of the experimental setup.

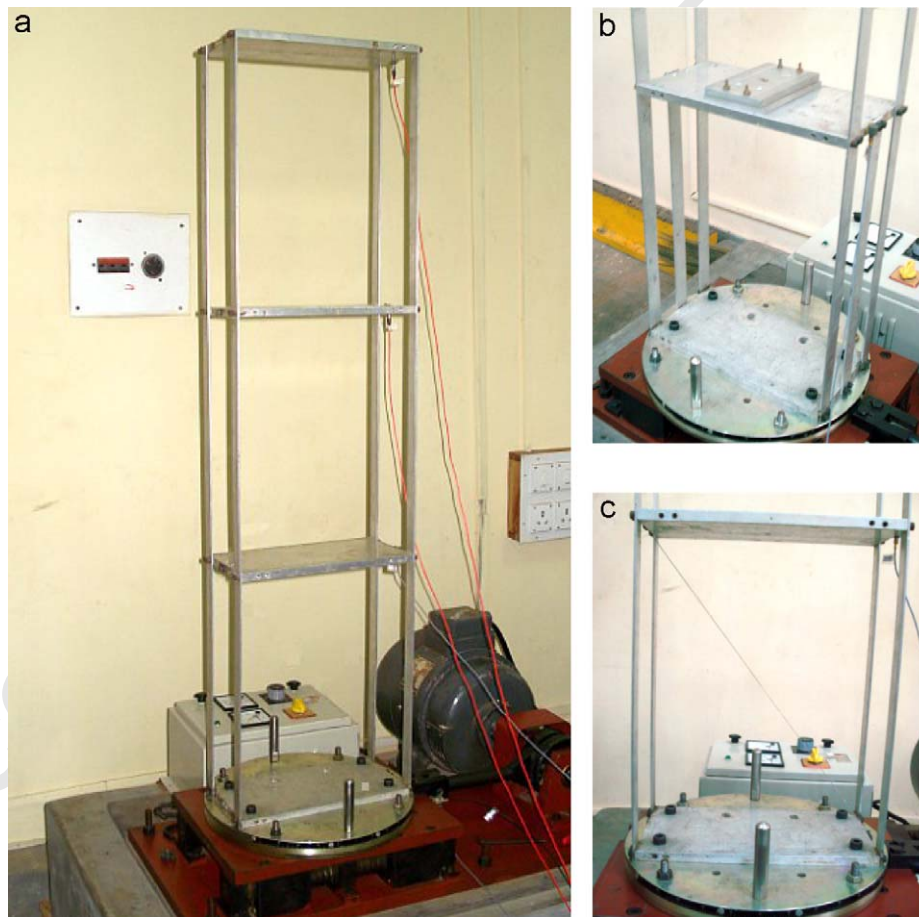


Fig. 16. Experimental models: (a) 3-storey building frame (model 0); (b) first storey of 'model 0' modified with additional columns and mass (model 1) and (c) first storey of 'model 0' attached with diagonal wires (model 2).

1 the presence of process and measurement noises in the system. A consistent reduction in the cumulative variance of the estimates is also evident. Thus, it is clear that the proposed filter yields accurate and variance reduced estimates. 3

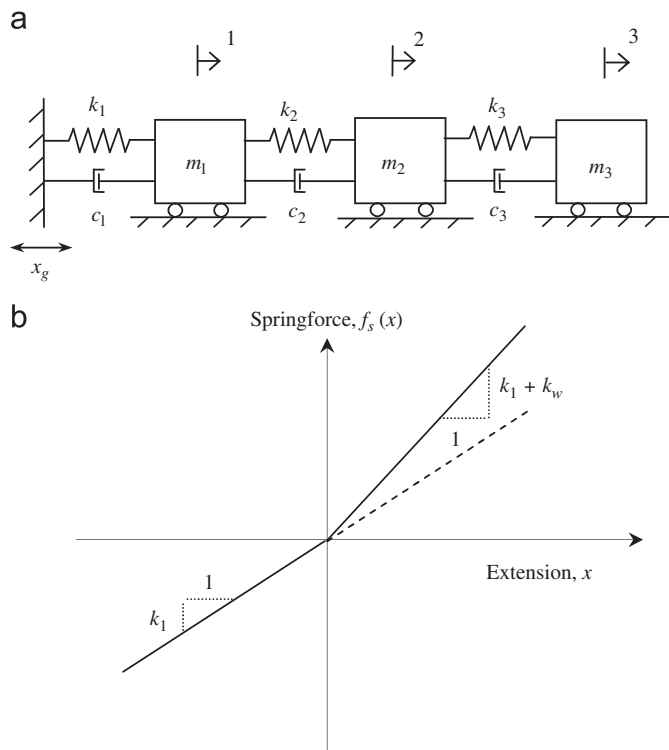


Fig. 17. (a) Analytical model of 'model 0' and (b) force–displacement relation of the first storey of 'model 2'.

4. An experimental validation

In this section, we study the problem of identification of system parameters based on laboratory experiments conducted on a 3-storey building frame (Figs. 15 and 16). Here the model structure is excited by harmonic base motion and the response of the floors (displacement, velocity or acceleration) could be measured using the sensors T₁–T₅. The experiments were conducted using standard vibration equipment and data acquisition system and these details indicated briefly in Fig. 15. In this study we first consider a reference model (Fig. 17a; designated as model 0) and we assume that its properties have been already identified by an independent means (such as, for instance, those based on experimental modal analysis or inverse sensitivity analysis). Newer structural models can now be generated by making suitable local modifications to this baseline model (models: 1 and 2; Figs. 17b and c). To obtain 'model 1', the first storey of 'model 0' was stiffened with two additional columns of the same type as used in 'model 0'. A mass of 0.511 kg was also added in the first floor slab. Fig. 16(b) shows the modifications made in the first storey of 'model 0'. Since no modification was done in the second and third stories of the basic frame, the mass, stiffness and damping parameters— m_2, m_3, k_2, k_3, c_2 and c_3 —of the model were assumed to be the same as those of 'model 0'. Next, 'model 0' was modified by attaching two steel wires of 0.25 mm diameter diagonally in the first storey as shown in Fig. 16(c) to obtain 'model 2'. The wires were attached in such a way that they were just taut in the undeformed state of the structure. Since the wires offer resistance in one direction only, the force–displacement relation of the first storey becomes bilinear (Fig. 17b). Thus 'model 2' is a non-linear frame with localized non-linearity in the first storey. The identification method proposed in this paper is applied to estimate the parameters of models 1 and 2.

Fig. 16a shows the 3-stoired building frame (model 0) that is made up of aluminum columns and slabs. The slab dimensions were 300.0 mm × 150.0 mm × 12.7 mm and the columns had rectangular

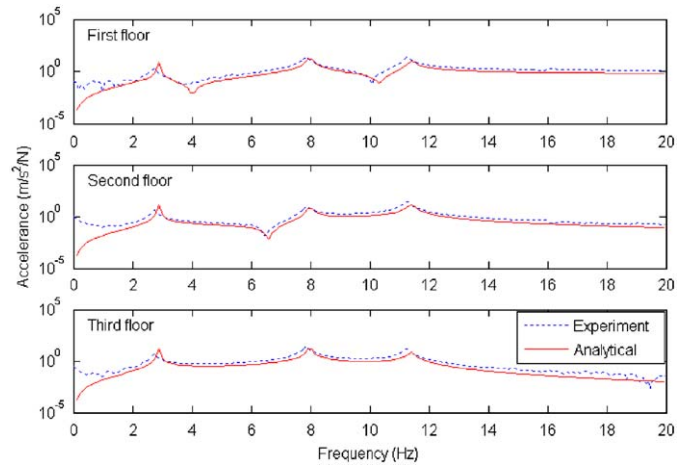


Fig. 18. FRFs (accelerations at different floors due to unit harmonic force at the second floor) of the 3-storey frame.

cross section of 25.1 mm × 3.0 mm. The floor heights were 400 mm. The behavior of this system can be adequately represented as a 3-DOF shear frame model (Fig. 17a) over a frequency range up to about 12 Hz [22]. The mass and stiffness parameters of the analytical model were estimated as $m_1 = m_2 = 1.8685$ kg, $m_3 = 1.7058$ kg; $k_1 = k_2 = k_3 = 2923.7$ N/m. In the present study a simple damping model of the frame was obtained by assuming it to be proportional to stiffness and the damping parameters are obtained as $c_1 = c_2 = c_3 = 0.65$ N s/m by minimizing the squared error between the experimental and analytical frequency response functions (FRFs). A fairly good match between the FRFs of the analytical model and those via experiments could be seen from Fig. 18. Figs. 19 and 20 show the experimental and calculated response (using the analytical model) of 'model 0' for harmonic base motions of frequencies 2 and 2.6 Hz (Figs. 19a and 20a), respectively. A good match between the experimental and numerically obtained responses (time histories of velocities of different floors—Figs. 19b and 20b) suggests that under low frequency harmonic base motions, the 3-DOF analytical model is adequate to represent the behavior of 'model 0'.

4.1. Experiments

The objective of the experiments is to estimate the unknown parameters in models 1 and 2, using the proposed filter, making use of the incomplete and noisy measurements. In 'model 1', we aim to estimate the stiffness and damping values of the first storey, whereas in 'model 2', the objective is to estimate the stiffness offered by the wires and the damping coefficient of the first storey. For comparison, estimations of the unknown parameters were done using the SIS filter also, using the same initializing parameters (initial pdfs of all states, parameters of process/measurement noise and ensemble size) as those used with the proposed filter. In both the experiments, measured velocities of the first and third floors were only used for estimating the parameters. Further details of the experiment are provided below.

4.1.1. Experiment on 'model 1'

The analytical model of 'model 1' could be represented by the model shown in Fig. 17(b), with m_1 modified as $m_1 + m_a$, where m_a represents the attached mass. The stiffness (k_1) and the damping coefficient (c_1) of the first storey of the modified frame were treated as the unknown parameters to be estimated and they are declared as additional states (x_7 and x_8 , respectively). The governing SDEs in

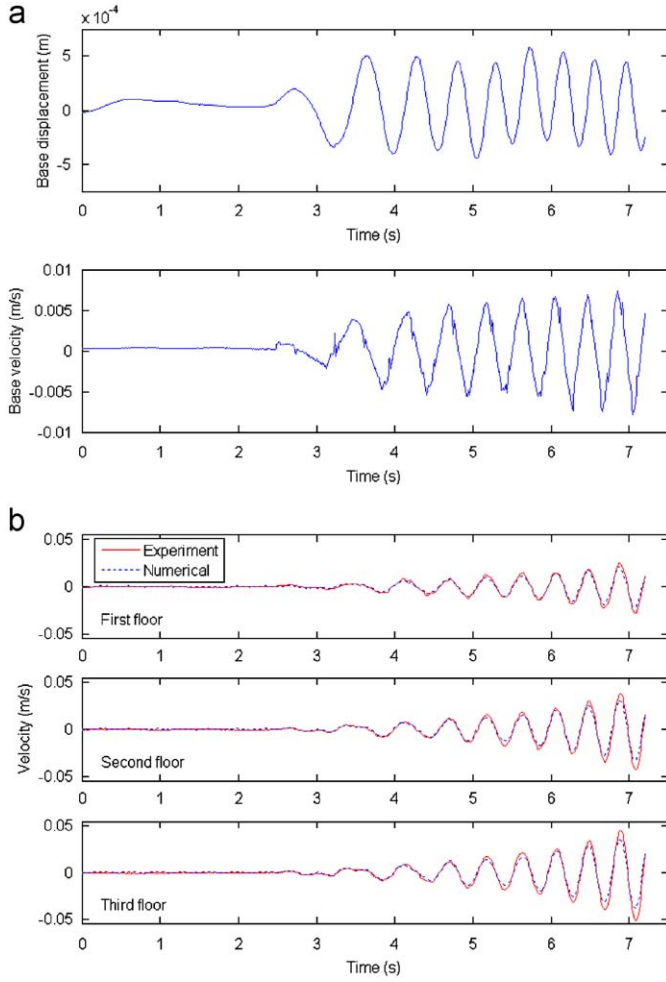


Fig. 19. Measured and calculated response of model 0 for harmonic base motion of frequency 2 Hz: (a) measured base motion and (b) velocity of floors.

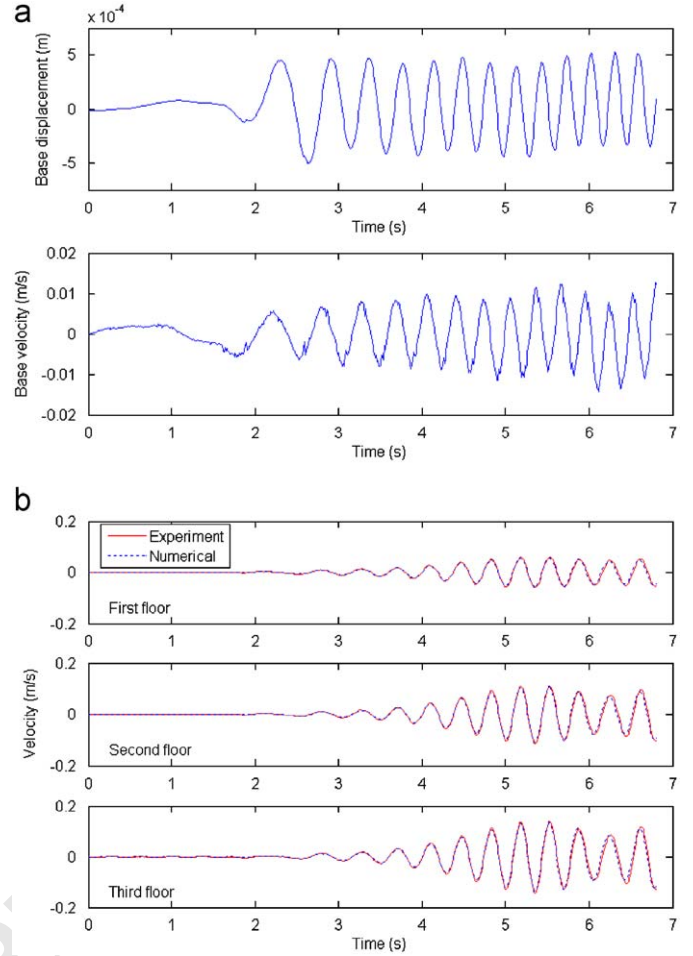


Fig. 20. Measured and calculated response of 'model 0' for harmonic base motion of frequency 2.6 Hz: (a) measured base motion and (b) velocity of floors.

1 incremental form may be expressed as

$$\left. \begin{aligned} dx_1 &= x_4 dt; & dx_2 &= x_5 dt; & dx_3 &= x_6 dt \\ dx_4 &= a_4 dt + \sigma_1 dB_1; & dx_5 &= a_5 dt + \sigma_2 dB_2; & dx_6 &= a_6 dt + \sigma_3 dB_3 \\ dx_7 &= \sigma_c dB_4; & dx_8 &= \sigma_k dB_5 \end{aligned} \right\} \quad (30)$$

3 with initial conditions $x_i(0) = x_{i0}$, $i \in [1, 8]$. The drift coefficients are obtained as

$$\left. \begin{aligned} a_4 &= -\frac{1}{m_1 + m_a} [x_8(x_1 - x_8) + x_7(x_4 - \dot{x}_g) + k_2(x_1 - x_2) + c_2(x_4 - x_5)] \\ a_5 &= -\frac{1}{m_2} [k_2(x_2 - x_1) + k_3(x_2 - x_3) + c_2(x_5 - x_4) + c_3(x_6 - x_5)] \\ a_6 &= -\frac{1}{m_3} [k_3(x_3 - x_2) + c_3(x_6 - x_5)] \end{aligned} \right\} \quad (31)$$

Here, σ_1, σ_2 and σ_3 are the intensities of the additive process noises. σ_c and σ_k represent the assumed diffusion coefficients associated with the parameter-states c_1 and k_1 , respectively. Since measured velocities of first and third floors were used in the estimation process, the measurement equations may be written as

$$\left. \begin{aligned} y_{1k} &= x_{4k} + v_{1k} \\ y_{2k} &= x_{6k} + v_{2k} \end{aligned} \right\} \quad (32)$$

where v_{1k} and v_{2k} represent measurement noises. Note that, given x_7 and x_8 , the process equation (30) becomes linear. If y_{1k} (in Eq. (32)) is taken as the observation for the particle filter, then \bar{x} (the states to be estimated using particle filter) may be marginalized

as $\bar{x} = [x_4; x_7; x_8]^T$. Conditioned on \bar{x} , linearized process equations may now be obtained as explained in Sections 2 and 3. Also, the discrete process equations for the particle filter may be arrived at using truncated Ito-Taylor expansions.

The process noise coefficients (σ_1, σ_2 and σ_3) were taken as 5% of the maximum absolute base acceleration. The standard deviation of the measurement noise (obtained by collecting the noise data using the setup used for measurement, with all the electronics switched on while keeping the structure at rest) was found to be 6×10^{-4} m/s. The initial pdf of x_7 (i.e., c_1) and x_8 (i.e., k_1) were assumed to be uniformly distributed in $[3000, 8000]$ N/m and $[0.75, 2.5]$ N s/m, respectively. The initial pdfs of all displacement and velocity states were, respectively, assumed as being uniformly distributed in $[-1 \times 10^{-4}, 1 \times 10^{-4}]$ m and $[-1 \times 10^{-3}, 1 \times 10^{-3}]$ m/s. The diffusion coefficients (σ_c and σ_k) of the parameter states were assumed to be 5% of the mean of their initial pdfs. An ensemble size of $N = 1500$ was used.

As has been done in the numerical study, in the experimental study also 100 independent MC simulations are performed to assess the sampling fluctuations in the estimation process. Fig. 21 shows the estimated velocities in one of the MC runs. Figs. 22 and 23 show, respectively, the mean and the cumulative variance of the estimated parameters over 100 MC runs. One trajectory of the estimated parameters, using the proposed filter, is also shown along with the mean of the estimated parameters. A fairly good convergence of the estimated states may be observed from Fig. 21. The value of the pa-

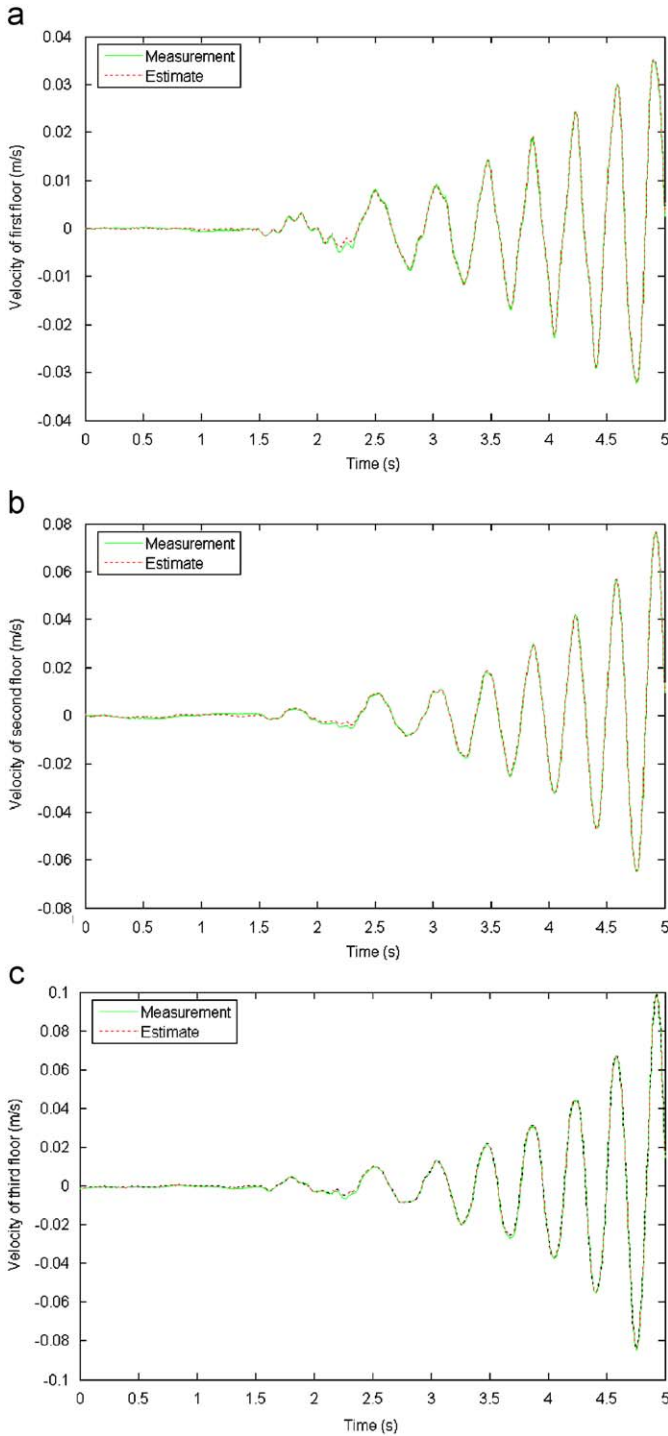


Fig. 21. Experiment on 'model 1'—estimated states in one of the MC runs: (a) velocity of first floor; (b) velocity of second floor and (c) velocity of third floor.

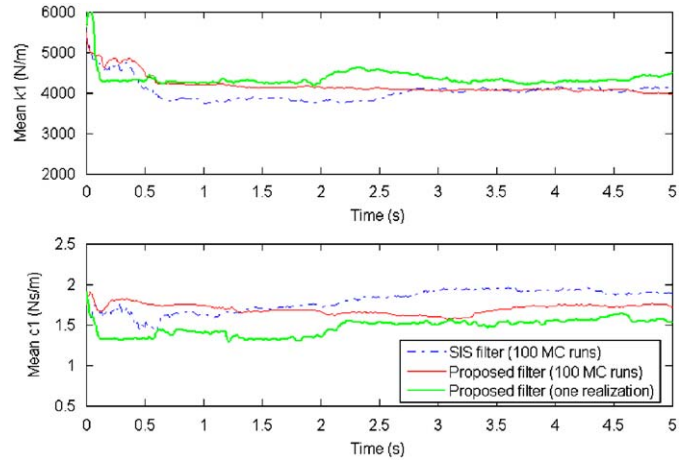


Fig. 22. Experiment on 'model 1'—estimate of parameters.

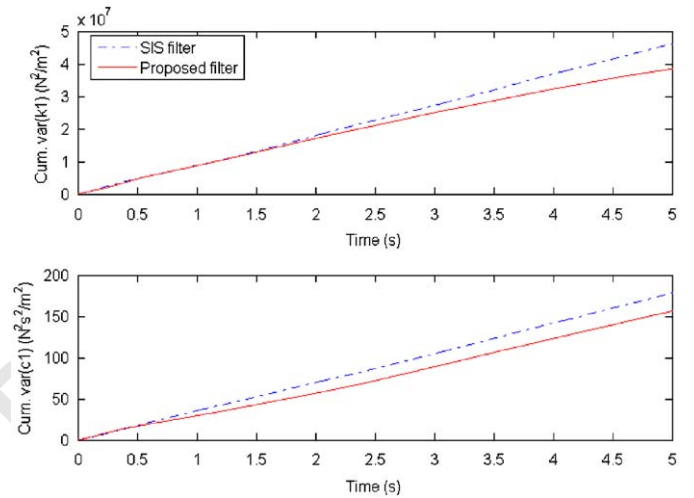


Fig. 23. Experiment on 'model 1'—cumulative sample variance of the estimated parameters.

tion, and compared with the actual response measured in the experiment (Fig. 24). It can be seen that the numerically obtained response matches reasonably well with the actual response obtained through the experiment, which shows the accuracy of the proposed estimation procedure.

4.1.2. Experiment on 'model 2

The analytical model shown in Fig. 17(b) could still be used to represent 'model 2', with the first linear spring (corresponding to the first storey) being replaced by a bilinear spring whose force-displacement relationship is as shown in Fig. 17(c). The force in the first spring may be written as

$$f_s(x) = k_1x \quad \text{if } x \leq 0$$

$$= (k_1 + k_w)x \quad \text{if } x > 0 \tag{33}$$

where k_w is the contribution of the wires to the stiffness of the first spring and x is the extension/contraction of the spring. Eq. (33) may be generalized as

$$f_s(x) = pk_1x + q(k_1 + k_w)x \tag{34}$$

where p and q are given by $p = 1, q = 0$ if $x \leq 0$ and $p = 0, q = 1$ otherwise.

parameter is calculated as the time-averaged mean of its estimate (in a single simulation) over the last 2 s of simulation. Thus, for the trajectories shown in Fig. 22, the values of k_1 and c_1 were found to be 4289.98 N/m and 1.54 N s/m, respectively. A reduction in the cumulative sample variance, through the proposed filter compared to SIS filter, can be observed in Fig. 23, which indicates that sampling fluctuations are less for the proposed filter. Making use of the values of k_1 and c_1 (as found above) in the analytical model of 'model 1' the response was obtained numerically, for a specific base mo-

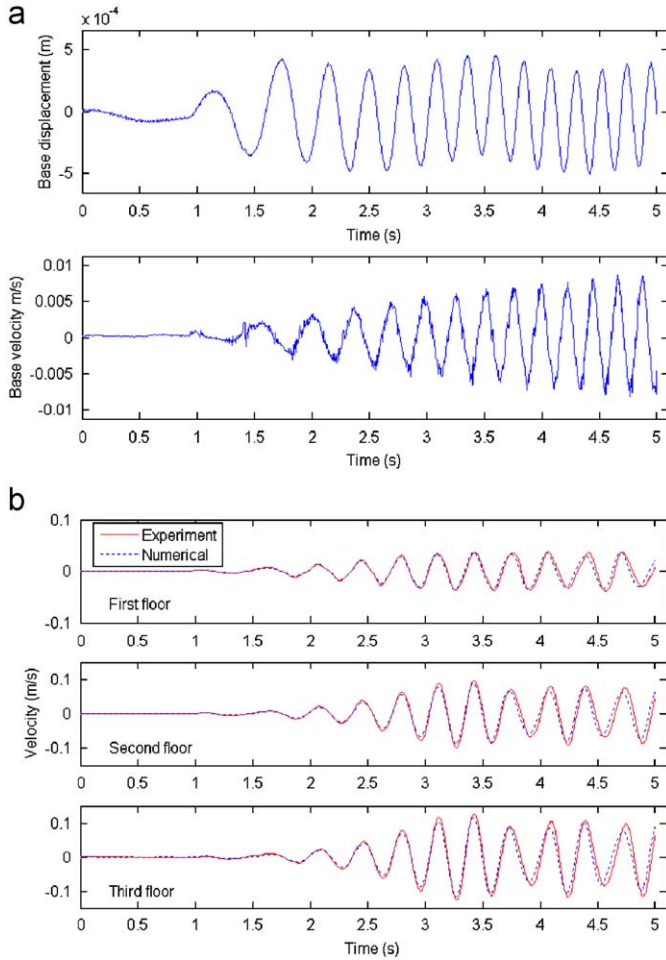


Fig. 24. Measured and calculated response of model 1 for a specific base motion: (a) measured base motion and (b) velocity of floors.

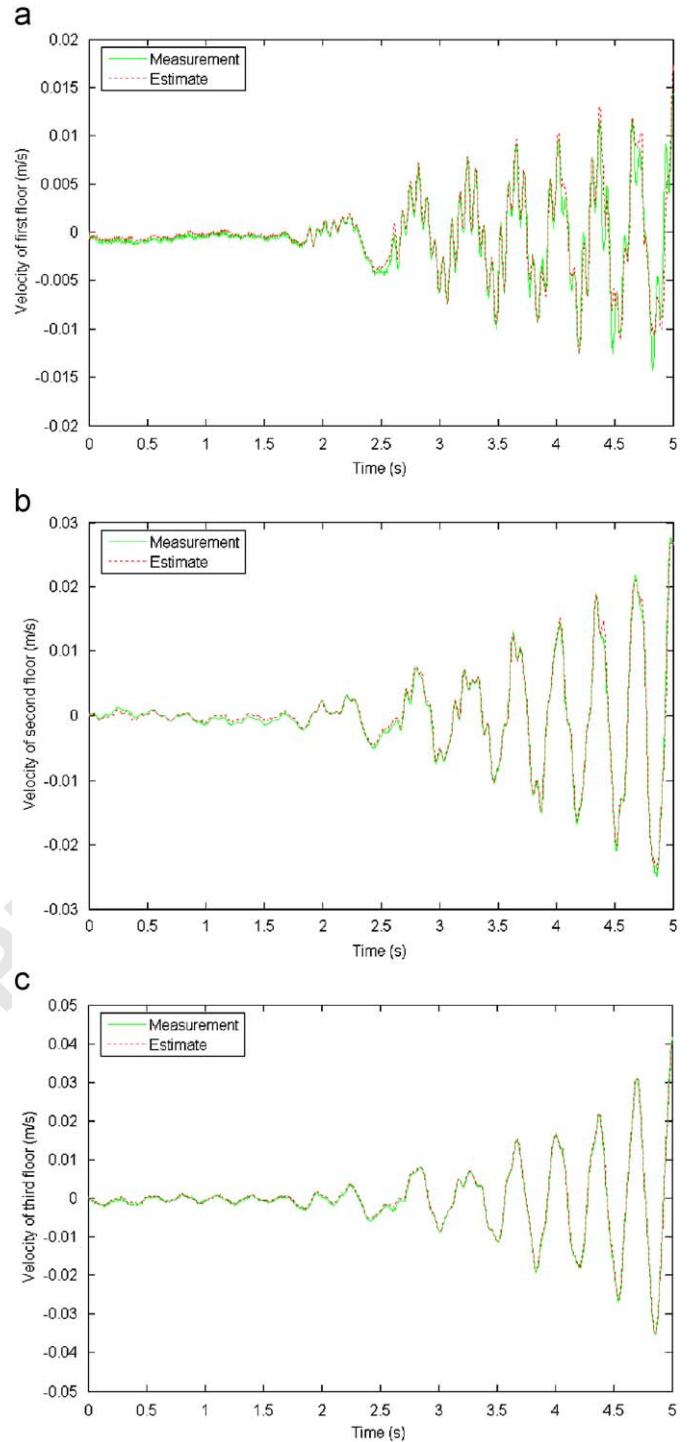


Fig. 25. Experiment on 'model 2'—estimated states: (a) velocity of first floor; (b) velocity of second floor and (c) velocity of third floor.

1 The damping coefficient of the first storey (c_1) and stiffness offered by the wires (k_w) are declared as additional states x_7 and x_8 , respectively. The governing SDEs of the system may be expressed in the following incremental form:

$$\left. \begin{aligned}
 dx_1 &= x_4 dt; & dx_2 &= x_5 dt; & dx_3 &= x_6 dt \\
 dx_4 &= a_4 dt + \sigma_1 dB_1; & dx_5 &= a_5 dt + \sigma_2 dB_2; & dx_6 &= a_6 dt + \sigma_3 dB_3 \\
 dx_7 &= \sigma_c dB_4; & dx_8 &= \sigma_k dB_5
 \end{aligned} \right\} \quad (35)$$

7 with initial conditions $x_i(0) := x_{i0}$, $i \in [1, 8]$. The drift coefficients are given by

$$\left. \begin{aligned}
 a_4 &= -\frac{1}{m_1} \{ [pk_1 + q(k_1 + x_8)](x_1 - x_8) + x_7(x_4 - \dot{x}_g) + k_2(x_1 - x_2) \\
 &\quad + c_2(x_4 - x_5) \} \\
 a_5 &= -\frac{1}{m_2} [k_2(x_2 - x_1) + k_3(x_2 - x_3) + c_2(x_5 - x_4) + c_3(x_6 - x_5)] \\
 a_6 &= -\frac{1}{m_3} [k_3(x_3 - x_2) + c_3(x_6 - x_5)]
 \end{aligned} \right\} \quad (36)$$

9 σ_1 , σ_2 and σ_3 are the intensities of additive process noises. σ_c and σ_k represent the assumed diffusion coefficients associated with the parameters c_1 and k_w , respectively. The measurement equations are the same as given in Eq. (32). Taking y_{1k} (Eq. (32)) as the observation for the particle filter, if one declares $\tilde{x} = [x_1; x_4; x_7; x_8]^T$, the process equation (35) becomes linear conditioned on \tilde{x} . The rest of the filtering algorithm follows the steps already outlined in Sections 2 and 3.

19 Towards estimating the unknown parameters, process and measurement noise intensities were taken the same as in experiment 1. An ensemble size of $N = 2500$ was used. The initial pdf of x_7 (i.e., c_1) and x_8 (i.e., k_w) are assumed to be uniformly distributed in $[8000, 28000]$ N/m and $[0.75, 3.0]$ Ns/m, respectively. The diffusion coefficients (σ_c and σ_k) of the parameter states were assumed to be 5% of the mean of their initial pdfs. The initial pdfs of the displacement and velocity states are also taken to be the same as those used in the previous experiment. The estimated floor velocities, obtained in

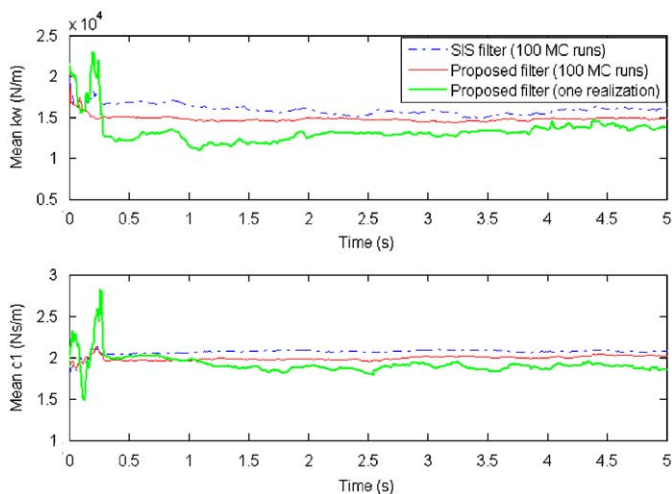


Fig. 26. Experiment on 'model 2'—estimate of parameters.

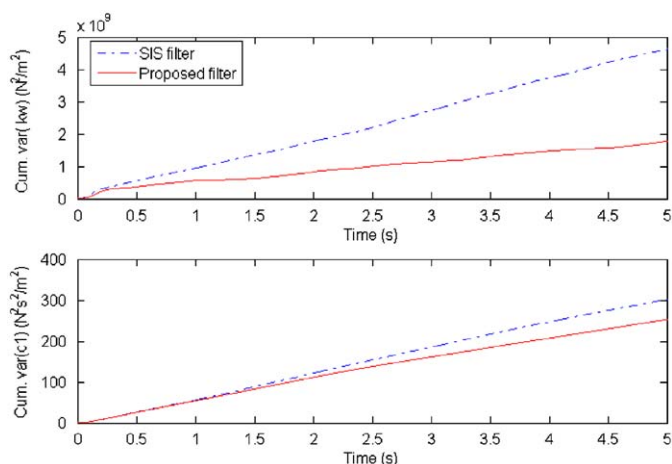


Fig. 27. Experiment on 'model 2'—cumulative sample variance of the estimated parameters.

one simulation, along with the respective measurements are shown in Fig. 25. The mean and the cumulative variance of the estimated parameters over 100 MC runs are shown in Figs. 26 and 27, respectively. Along with the mean of the estimated parameters, one trajectory of the estimated parameters, using the proposed filter, is also shown. From Fig. 25, one may observe that the estimated velocities of second and third floors converge reasonably well whereas convergence of the estimated velocity is slightly inferior for the first floor. In this case also, compared to the SIS filter, the proposed filter results in less cumulative variance of the estimated parameters (Fig. 27). From the estimated trajectories of the parameters the values of k_w and c_1 were obtained as 13511 and 1.89 N s/m, respectively. With these values used in the analytical model, the response of 'model 2' was obtained numerically, for a given base motion (Fig. 28a), and compared with the measured response obtained in the experiment (Fig. 28b). A satisfactory comparison between the numerical and experimental response is indicative of the accuracy of the proposed method in parameter identification.

5. Concluding remarks

A conditionally linearized Monte Carlo filter for state and parameter estimations of non-linear structural dynamical systems with

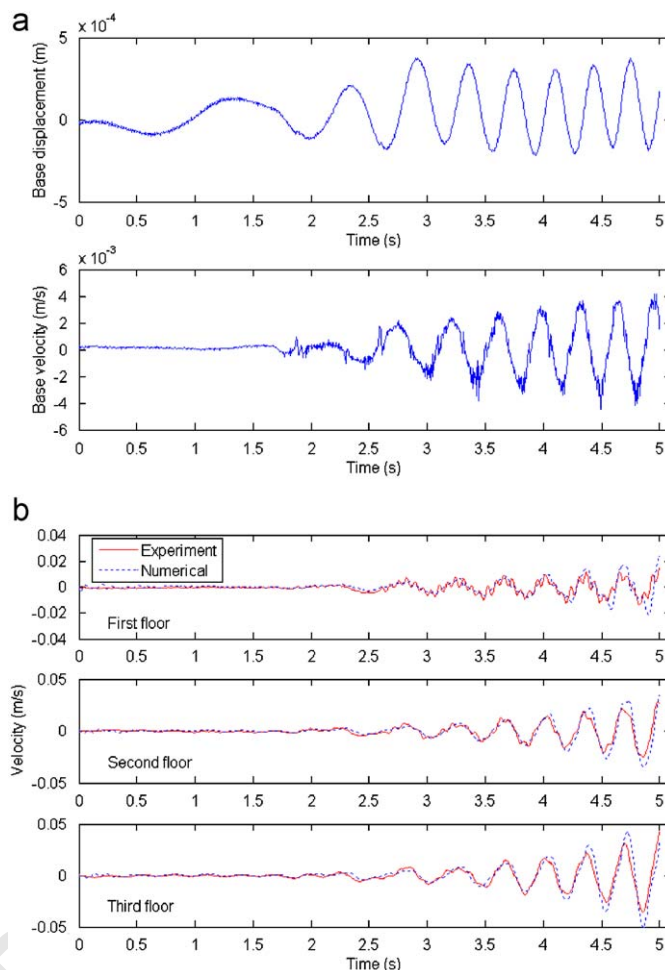


Fig. 28. Measured and calculated response of 'model 2' for a specific base motion: (a) measured base motion and (b) velocity of floors.

Gaussian additive noises is proposed. A small (marginalized) subset of the state vector, which contains the system states appearing in the non-linear functions in the process equations and (some of the) measurement equations, is estimated using a particle filter and the resulting information is used to linearize the system equations. The system states are then estimated using a bank of Kalman filters. As the number of states to be estimated via the particle filter increases with the number of states involved in the system non-linearity, the proposed method is considered ideal for large systems with localized non-linearity. In addition to a reduction in the sample variance of the estimate, the present method also eases the discretization requirements of the governing SDEs. Discrete maps of the marginalized states (to be estimated through the particle filter) only need to be obtained using stochastic Taylor expansions. Limited numerical illustrations on a few non-linear oscillators and experimental demonstrations on laboratory models are indicative of the superior performance of the proposed method. While the method is computationally expensive, the focus of this study has been on an exploration of techniques to increase the analyticity of the filtering schemes and to study the sampling fluctuations of the resulting algorithm. As a consequence of a substantial amount of calculations being done analytically in arriving at the conditional pdf, the variance of the estimator is found to be reduced vis-à-vis the standard SIS filter. However, further studies are essential for rigorous analyses of the sampling fluctuations and convergence characteristics.

1 **6. Uncited reference**

[18].

3 **Acknowledgment**

C.S.M. thanks the Aeronautical R&D Board, Government of India, for the financial support provided to conduct a part of this work.

References

- 5 [1] R.G. Brown, P.Y.C. Hwang, Introduction to Random Signals and Applied Kalman
Filtering, Wiley, New York, 1992.
- 7 [2] J. Ching, J.L. Beck, K.A. Porter, Bayesian state and parameter estimation of
uncertain dynamical systems, Probabilistic Engineering Mechanics 21 (2006)
81–96.
- 9 [3] J. Ching, J.L. Beck, K.A. Porter, R. Shaikhutdinov, Bayesian state estimation
method for nonlinear systems and its application to recorded seismic response,
Journal of Engineering Mechanics—ASCE 132 (4) (2006) 396–410.
- 11 [4] N. Chopin, Central limit theorem for sequential Monte Carlo methods and its
application to Bayesian inference, Annals of Statistics 32 (2004) 2385–2411.
- 13 [5] D. Crisan, A. Doucet, A survey of convergence results for particle filtering
methods for practitioners, IEEE Transactions on Signal Processing 50 (2002)
736–746.
- 15 [6] A. Doucet, On sequential simulation-based methods for Bayesian filtering,
Technical Report CUED/F-INFENG/TR.310 (1998), Department Electrical
Engineering, University of Cambridge, UK.
- 17 [7] A. Doucet, S. Godsill, C. Andrieu, On sequential Monte Carlo sampling methods
for Bayesian filtering, Statistics and Computing 10 (2000) 197–208.
- 19 [8] A. Doucet, N. de Freitas, N. Gordon, Sequential Monte Carlo Methods in Practice,
Springer, New York, 2001.
- 21 [9] R. Ghanem, M. Shinozuka, Structural system identification I: theory, Journal of
Engineering Mechanics—ASCE 121 (1995) 255–264.
- 23 [10] S.J. Ghosh, D. Roy, C.S. Manohar, New forms of extended Kalman filter via
transversal linearization and applications to structural system identification,
Computer Methods in Applied Mechanics and Engineering 196 (2007) 5063–
5083.
- 25 [11] S.J. Ghosh, C.S. Manohar, D. Roy, A sequential importance sampling filter with
a new proposal distribution for state and parameter estimation of nonlinear
dynamical systems, Proceedings of the Royal Society A 464 (2008) 25–47.
- 27 [12] N.J. Gordon, D.J. Salmond, A.F.M. Smith, Novel approach to nonlinear/non-
Gaussian Bayesian state estimation, IEE Proceedings—F 140 (1993) 107–113.
- 29 [13] H. Imai, B. Yun, O. Maruyama, M. Shinozuka, Fundamentals of system
identification in structural dynamics, Probabilistic Engineering Mechanics 4
(1989) 162–173.
- 31 [14] R.E. Kalman, A new approach to linear filtering and prediction problems,
Transactions of the ASME—Journal of Basic Engineering 82 (Series D) (1960)
35–45.
- 33 [15] G. Kerschen, G.K. Worden, A.F. Vakakis, J.C. Golinval, Past, present and future
of nonlinear system identification in structural dynamics, Mechanical Systems
and Signal Processing 20 (2006) 505–592.
- [16] P.E. Kloeden, E. Platen, Numerical Solution of Stochastic Differential Equations, 45
Springer, Berlin, 1992.
- [17] J.H. Kotecha, P.M. Djuric, Gaussian particle filtering, IEEE Transactions on Signal 47
Processing 51 (2003) 2592–2601.
- [18] J.H. Kotecha, P.M. Djuric, Gaussian sum particle filtering, IEEE Transactions on 49
Signal Processing 51 (2003) 2602–2612.
- [19] S.J. Li, Y. Suzuki, M. Noori, Improvement of parameter estimation for non-linear 51
hysteretic systems with slip by a fast Bayesian bootstrap filter, International
Journal of Nonlinear Mechanics 39 (2004) 1435–1445.
- [20] J.S. Liu, Monte Carlo Strategies in Scientific Computing, Springer, New York, 53
2001.
- [21] C.S. Manohar, D. Roy, Monte Carlo filters for identification of nonlinear structural 55
dynamical systems, Sadhana—Academy Proceedings in Engineering Sciences,
Indian Academy of Sciences 31 (4) (2006) 399–427.
- [22] C.S. Manohar, S. Venkatesha, Development of experimental setups for 57
earthquake engineering education, Report National Program on Earthquake
Engineering Education, MHRD, Government of India, 2006, submitted for
publication.
- [23] R.V. Merwe, A. Doucet, N. de Freitas, E. Wan, The unscented particle 61
filter, Technical Report, CUED/F-INFENG/TR.380, Department of Engineering,
University of Cambridge, UK, 2000.
- [24] G.N. Milstein, Numerical Integration of Stochastic Differential Equations, Kluwer 65
Academic Publishers, Dordrecht, 1995.
- [25] B. Oksendal, Stochastic Differential Equations: An Introduction with 69
Applications, Springer, Berlin, 1992.
- [26] A. Papoulis, S.U. Pillai, Probability, Random Variables, and Stochastic Processes, 71
Tata McGraw-Hill, New Delhi, 2002.
- [27] B. Ristic, S. Arulampalam, N. Gordon, Beyond the Kalman Filter—Particle Filters 73
for Tracking Applications, Artech House, Boston, London, 2004.
- [28] C.P. Robert, G. Casella, Monte Carlo Statistical Methods, second ed., Springer, 75
New York, 2004.
- [29] D. Roy, A family of lower- and higher-order transversal linearization 77
techniques in non-linear stochastic engineering dynamics, International Journal
of Numerical Methods in Engineering 61 (2004) 764–790.
- [30] D. Roy, A new numerical-analytical principle for nonlinear deterministic and 79
stochastic dynamical systems, Proceedings of the Academy of the Royal Society
(London) 457 (2001) 539–566.
- [31] E. Saito, M. Hoyshiya, Structural identification by extended Kalman filter, Journal 81
of Engineering Mechanics—ASCE 110 (1984) 1757–1770.
- [32] R. Sajeeb, C.S. Manohar, D. Roy, Rao-Blackwellization with substructuring for 83
state and parameter estimations of a class of nonlinear dynamical systems,
International Journal of Engineering under Uncertainty: Hazards, Assessment
and Mitigation (2008), submitted for publication.
- [33] H. Tanizaki, Nonlinear Filters: Estimation and Applications, Springer, Berlin, 85
1996.
- [34] H. Tanizaki, R.S. Mariano, Nonlinear and non-Gaussian state-space modeling 87
with Monte Carlo simulations, Journal of Econometrics 83 (1998) 263–290.
- [35] V. Namdeo, C.S. Manohar, Nonlinear structural dynamical system identification 91
using adaptive particle filters, Journal of Sound and Vibration 306 (2007) 524
–563.